GEOCHEMICAL IMPACT OF SUPER-CRITICAL CO_2 INJECTION INTO THE ST. PETER SANDSTONE FORMATION WITHIN THE ILLINOIS BASIN: IMPLICATION FOR STORAGE CAPABILITY IN A CARBON DIOXIDE SEQUESTRATION SYSTEM

Richard Michael Thomas

Submitted to the faculty of the University Graduate School
in partial fulfillment of the requirements
for the degree
Master of Science
in the Department of Earth Sciences,
Indiana University

June 2014

Accepted by the Faculty of Indiana University, in partial
fulfillment of the requirements for the degree of Master of Science.

Master's Thesis Committee

Gabriel M. Filippelli Ph.D., Chair

John A. Rupp M.Sc., Indiana Geological Survey

Kevin W. Mandernack Ph.D.

ACKNOWLEDGMENTS

Gabe Filippelli, John Rupp, Kevin Mandernack

Kevin Strunk, Lauren Thomas, Fei Wang, Rosalice Buhrer

Richard Michael Thomas

GEOCHEMICAL IMPACT OF SUPPER CRITICAL CO_2 INJECTION INTO THE ST. PETER SANDSTONE FORMATION WITHIN THE ILLINOIS BASIN

Deep injection of waste CO_2 and fluids from regional energy plants into the St. Peter Formation of the Illinois Basin, could effectively provide long term deep geologic storage. This research aims to explore the viability of this proposed injection. There are some basic criteria that must be met to effectively store waste in a geologic reservoir.

First, the reservoir must have sufficient porosity and permeability for both injectivity and for migration of the injected fluid through the reservoir. Second, the reservoir must be overlain by some form of impermeable seal or cap layer(s). Third, the reservoir should be sufficiently isolated from interaction with surface and near surface water. Finally, the formation must contain enough storage volume to handle significant amounts of injected material.

Massive sandstone formations that host large saline aquifers have the potential to serve as high capacity storage sites. Much of the research targeting the potential suitability and storage capacity attributes of these formations has been promising, but reproducibility of the results has been less than ideal. Some of this variability has been attributed to petrological differences in the sandstone reservoirs that are not readily evident when studying the target formation over a geographically significant area.

Based on the criteria, a promising candidate for injection and storage is the St. Peter Sandstone of the Illinois Basin. This study investigates the viability of liquefied CO_2 storage within the St. Peter Sandstone on a micro scale.

Initial porosity and permeability of the formation plug samples ranged from 16% to 19% and 26 to 981 millidarcies (mD), respectively. The wide difference in permeability is attributed to variations in strength of the cement, in this case quartz overgrowth in the sandstone. This preliminary evidence indicates that the storage capacity of the formation will remain constant or increase depending on injection location, suggesting that the St. Peter Formation will lend itself well to future storage.

Gabriel M. Filippelli Ph.D., Chair

TABLE OF CONTENTS

LIST OF FIGURES

INTRODUCTION

1.1 Carbon Sequestration

The buildup of carbon dioxide (CO_2) and other greenhouse gases in the atmosphere as a result of human activities is changing the composition of the Earth's atmosphere and warming the planet. Studies link these atmospheric changes to a range of surface impacts, including shrinking glaciers, sea level rise, shifts in plant and animal habitats, and other global impacts. The Intergovernmental Panel on Climate Change (IPCC) identified CO_2 capture and geologic sequestration as one of several options (including energy efficiency and renewable energy) that have the potential to reduce climate change mitigation costs and increase flexibility in achieving greenhouse gas emission reductions (Metz et al, 2010). The IPCC estimates that there is enough capacity worldwide to permanently store as much as 1,100 gigatons of CO_2 underground - for reference, worldwide emissions of CO_2 from large stationary sources is approximately 13 gigatons per year (Benson et al, 2005).

There have been several methods proposed for carbon sequestration. One of the more appealing is geological storage/sequestration. The appeal for this method can be attributed to the fact that much of the technology and research used for this form of sequestration has already been developed over the past decades by the oil and gas industry. Geological storage of CO_2 involves capture and separation of the CO_2 from a hydrocarbon burning power plant and then injecting that captured CO_2 into deep subsurface reservoirs such as depleted hydrocarbon reservoirs, un-mineable coal seams or saline aquifers with sufficient permeability and porosity to enable efficient injection

and storage. The reservoirs must also have the pressure and temperature to maintain the injected CO_2 in the super critical state. Deep saline aquifers are far more common and widespread than hydrocarbon reservoirs or coal seams (Kaszuba et al, 2005). Saline aquifers form when carbonic acid from atmospheric CO2 interacts with the rock. The resulting ions/salts are retained in the water and increase the salinity over thousands of years. This availability of storage location and capacity reduces the need for transportation thereby reducing overall transportation expense. The massive sandstone formations that are the hosts for large saline aquifers have the potential to serve as high capacity storage sites (fig. 1).

Much of the research targeting these formations has been promising. The Midwest Regional Carbon Sequestration Partnership has determined that saline aquifer formations in the Midwest, such as the St. Peter and Mount Simon Sandstone, have good storage potential for CO_2 emissions captured from stationary sources in the region (Bachu, 2009). Initial test results from The Mount Simon, described as a basal Cambrian formation in the upper Mississippi Valley (Indiana Geological Survey, 2013), indicate good permeability and injectivity with injection rates up to about 1,200 metric tons per day (MRCSP, 2011). However, success in one geologic formation does not guarantee success in another. The reactions that occur may be highly site specific and depend on the geochemical conditions and minerals in the formation rock (Bentham, 2005). Prediction of these reactions is best constrained by geochemical experiments using physical samples of the specific rocks (Bentham, 2005). Another reason for site-specific geochemical analysis is to determine how rock dissolution changes the porosity and

permeability of the host formation. The effective permeability and porosity of the near-well region are likely to decrease with time as salts are deposited when injected CO_2 migrates through the injected or resident saline water. Conversely, in a carbonate aquifer the injected CO_2 will dissolve the aquifer rock in the near-wellbore region and increase the porosity and permeability. (Mijic, 2012) This is beneficial for injection rate, but could cause wellbore failure if a substantial fraction of the limestone and cement are dissolved at the wellbore. Moreover, observations in fractured systems show that the dissolution/precipitation reaction of limestone and CO_2 tends to enhance the preferential flow paths, which could cause channeling of CO_2 and lead to poor storage efficiency in the long run. The competition between salt precipitation and carbonate dissolution will determine whether it gets easier or harder to inject CO_2 with time (Mijic, 2012). However there is also information showing that the drop off in pH created by the $SCCO_2$ injection decreases carbonate formation (Liu et al, 2010). To facilitate the amount of carbonate formation that would lead to effective CO_2 sequestration, buffering solutions would need to be injected as well (Liu et al, 2010).

It is therefore vital that geochemical analysis be conducted for the prospective reservoir at each candidate site. The St. Peter Sandstone in the Illinois Basin is located geographically close to numerous coal fired electric plants in the region, which are significant producers of CO_2 emissions (Schaper, 2011) (fig. 2). The targeted site in the St. Peter is located in Southeastern Illinois.

The shallower depth of the St. Peter (1600-2400 mbsf) could serve to further reduce the cost associated with well construction compared to the Mount Simon

(maximum depth of 4250 mbsf) (Hoholick, 1980; Pollington, 2011). Although the major cost of CO_2 injection involves the capture process, as much as 80% in some scenarios (Stephens, 2009), well depth is still an important factor in site selection, given it is closely associated with the cost (RISC, 2009).

1.2 Regional Geology

The Illinois Basin is an elongate intracratonic basin located mostly in central and southern Illinois, southwestern Indiana, and western Kentucky (Collinson et al, 1988). It extends some 600 km northwest to southeast and 320 km northeast to southwest. A maximum thickness of 7,000 meters of Paleozoic sedimentary fill is in southern Illinois and western Kentucky (Strąpoć et al, 2007) (fig. 3).

Within Indiana, the Middle Ordovician St. Peter Sandstone is a regionally continuous, porous and permeable sandstone (Droste et al, 1982) In the southern Illinois Basin the St. Peter ranges in thickness from 31 to 50 feet (Warne, 2012) (fig. 13d) and is overlain by the thick, impermeable, regionally extensive Black River Group, Trenton Limestone, and Maquoketa Group, (Droste, 1982) (fig. 14) which serves as an aquiclude (Young, 1992). The depositional environment of the St. Peter is much debated. Original depositional theories proposed a primarily eolian environment noting the dominant fine grain size, excellent sorting, rounding and frosting as well as its craton-wide extent (Berkey, 1906; Grabau, 1913). However, further characterization indicates both eolian and marine origin (May, 1985). It is likely a combination of both, beginning as a massive dune field that was overtaken and reworked by a marine transgression (that is, transgressive barrier bar sequence) and transformed into a series

of offshore bar deposits (Missouri DNR, 2009). Major diagenetic events modifying the St. Peter include: mechanical compaction, early K-feldspar overgrowth and dolospar precipitation burial quartz, dolospar, anhydrite, and calcite cementation and finally carbonate-cement and K-feldspar grains (Barnes, 1992).

Radiometric age dates of authigenic K-feldspar and illite in combination with the reconstructed burial history of the St. Peter reveal that early-diagenetic K-feldspar and dolospar precipitated at shallow to moderate depths in the Devonian, whereas late-diagenetic quartz, dolospar, anhydrite, and calcite formed during deep burial in the Late Pennsylvanian to Early Permian (Pitman, 1997). Stable-isotope geochemistry and fluid-inclusion paleothermometry suggest that burial cements precipitated from saline fluids over a wide temperature range. In the southern part of the basin, burial cements preserve a record of diagenetic effects that were in part controlled by fractures and hydrothermal-fluid circulation. Baroque dolospar cementation is the most significant of these effects (Pitman, 1997).

The deeper portions of the Illinois Basin were the focus of this investigation because this area contains strata that are sufficiently deep, porous and permeable, and hydraulically isolated from fresh-water aquifers to make potential CO_2 sequestration targets. Moreover, southern Illinois and western Kentucky are areas containing major CO_2 producing power plants (Warne, 2012).

The subsurface of this area has been well studied, but the majority of the research has focused on shallow, fresh water aquifers and hydrocarbon horizons. There are only a few brine-aquifer waste-disposal studies in the region (Bergstrom, 1968;

Cartwright et al, 1981; Roy et al, 1988). However much of this has been focused on the Mt. Simon Formation because of its larger sink capacity of approximately 5.9 billion tons. The St. Peter has a sink capacity of approximately 1.9 billion tons (Leetaru et al, 2005). Similar research concerning the St. Peter Formation will enable a more complete picture of the CO_2 storage potential within The Arches Province.

ANALYTICAL METHODS

Four one-inch representative plugs were obtained from the Indiana Geological Survey Core Depository. These plugs were used pre-reaction and post-reaction analysis to determine the impact of $SCCO_2$ injection into the St. Peter Formation.

Petrographic Analysis: Pre and post reaction samples were subjected to a petrographic analysis to describe the structure, framework, cement and pore type. This enabled changes in these attributes as a result of the reaction with $SCCO_2$ to be quantified.

Mineralogical Analysis: Geochemical analysis was performed on the brine used in the reaction both during and after the reaction. This data was used to determine brine-rock reactions. X-Ray Diffraction Analysis was performed on pre and post reaction plug samples to determine changes in rock composition, specifically what precipitates were formed.

Petrophysical Analysis: Pre-reaction analysis was done to determine pore volume and porosity of the plugs. This was data provided a baseline to compare differences between pre and post reaction porosity and permeability

2.1 Sample Collection

To this point, the St. Peter Formation has been well studied as a source of fresh water for municipal and industrial use. However much of this work has been in the shallower sections of the basin with few wells penetrating the deeper sections targeted in this research (Warne, 2012). Sample collection has been limited to wells with cores through at least a portion of the St. Peter. Samples for this study were taken from

existing cores of the St. Peter Formation and were obtained from the Indiana Geological Survey. These cores were one inch in diameter and ranged from five to twelve inches in length. Cores were obtained from the core depository located within the Indiana Geological Survey. The well and core information is as follows:

	Sample B129 and B131	Sample B137 and B139
Core box number:	790	807
Operator:	St. Joe Lead	St. Joe Lead
IGS ID:	158080	159300
County:	Fulton	Starke
Sct, Twp, Rng:	26, 30N, 1E	32, 32N, 1W
Well name:	Frettinger	Heise, Edward
Well number:	80 IN-4	80 IN-1

Both Fulton and Starke County are located in northern Indiana (fig. 4-5), along the Kankakee Arch on the eastern edge of the Illinois basin. Data collected from these samples included 16 thin sections, 2 inductively coupled plasma mass spectrometry analysis, and 16 x-ray diffractograms. Given the homogeneity of the formation, the samples analyzed provided an effective first look regarding possible CO_2 storage in the St. Peter Formation in the Illinois Basin.

2.2 Petrographic Analysis

To enable petrographic analysis and comparison within the St. Peter Formation, thin sections of each of the four core samples were examined at 40, 100 and 400 times magnification using a Leitz Labrolux 11 polarizing optical microscope both before reaction and after reaction with super critical CO_2. Because of the weakly cemented nature of samples B129 and B137 pre-reaction petrology analysis was performed on these two samples by CoreLab LLC in Houston Texas. All thin sections were prepared by first impregnating the samples with epoxy to augment cohesion and to prevent loss of material during grinding. The thinly sliced samples were each mounted on a glass slide, then cut and ground in water to an approximate thickness of 30 microns. All thin sections were analyzed using standard petrographic techniques. Figure 6 shows hand sample image alongside pre-reaction porosity, permeability, and grain density and location information. The results of the petrographic analysis are shown in Figure 7 which contains information about the structure, framework, cement and pore type as well as detailed sample descriptions.

2.3. Mineralogical Analysis

Geochemical and X-Ray Diffraction Analysis was performed to determine changes to brine and sample composition as a result of $SCCO_2$ injection. Geochemical analysis of the brine before, during and after reaction offered the ability to measure reaction time and the formation of precipitates. X-Ray Diffraction analysis measured secondary mineral development in the sample as a result of the $SCCO_2$ injection.

2.3.1 Geochemical Analysis

CO_2 becomes super-critical at 31.1°C and 73.8bar (Jessop & Leitner, 1999) (fig. 8). This combination of temperature and pressure is found in the St. Peter in the Southeastern Illinois region (Kinney, 1976 and Warne, 2012) (fig. 13: a-c). Elemental analysis of brines from two of the four pre-reacted samples was made by ICP (fig. 9). The reaction brine was synthesized using the compositional description of St. Peter brine (Keller, 1983). Composition of the synthesized brine was verified using ICP Mass Spectroscopy in the geochemistry department at Indiana University – Purdue University Indianapolis. The elements measured in the ICP analysis reflect the composition of the brine where possible (fig. 9).

Brine – rock – $SCCO_2$ reactions were performed on sample B129 and B137 at Washington University in St. Louis Missouri. Only two of the four samples were used due to constraints on the availability of the test rig. Sample size for each was 1” in diameter x ¾” long. Each sample was placed in an individual 200ml PTFE liner cup with 180ml of the synthetic brine. The liner cups were then placed in individual Parr reaction vessels that were ported to allow real time $SCCO_2$ injection and a spigot to allow in situ brine sampling at hours 0, 4, 8, 24, 72, 168-(7day) and 336-(14 day). Each sample taken was 5mL, filtered through a single use Millipore filter and tested for pH. The sample then received micro liters of 1% Nitric acid to stabilize and moved to a sealed vial. During the reaction pressure was maintained at 84 bar using a CO_2 pump and temperature at 70°C using a water bath. Real time analysis enabled estimation of reaction time as well as monitoring secondary mineral development specifically changes

in the trace K-feldspar found in the samples. This secondary mineral development could indicate what mineral trapping mechanisms the St. Peter Formation offers for the long-term geologic storage of CO_2.

2.3.2. X-Ray Diffraction Analysis

X-ray diffraction patterns were collected on all samples gathered from the St. Peter Formation. Pre and post reaction diffractograms were obtained from pressed powders of each bulk sample using a Siemens X-ray diffraction system in the geochemistry department at Indiana University-Purdue University Indianapolis. Each of the samples was analyzed twice by XRD before and after the reaction for a total of 16 diffractograms. Each diffractogram consist of the average of 10 individual XRD runs. The first eight diffractograms consist of pre and post reacted samples scanned from 10^{o} to 80^{o} 2θ with a 0.050^{o} step and a 2.4 sec step time. This scan window was used to confirm primary composition and determine any large-scale mineralogical changes in the sample during reaction. The final eight diffractograms consist of pre and post reacted sample scanned from 29^{o} to 36^{o} 2θ with a 0.010^{o} step and a 2.4 sec step time. This scan window was used to focus on possible peaks caused by carbonate development that occurred during reaction. The data was then analyzed using the Crystal Sleuth software package for d-spacing values. This data is considered semi-quantitative due to the fact that it is using peak intensities instead of peak/profile areas.

2.4 Petrophysical Analysis

Pre-reaction petrophysical analysis was performed by Core Labs LLC, Houston Texas at their Advanced Technology Center to determine pre-reaction pore volume and porosity.

High pressure mercury injection was used in establishing pore volume and porosity in our samples. Mercury is an extremely non-wetting material and must be forced with pressure to conform around and into surface features (Core Laboratories, 2012) enabling accurate measure of pore volume and porosity across different mineral and rock types.

1. Testing was performed using the Micromeritics Autopore 9320, an automated, high pressure mercury injection device which operates at injection pressures of 0 to 55,000 psia.

2. Each rock sample was weighed, and then loaded into a glass penetrometer consisting of a sample chamber attached to a capillary stem with a cylindrical coaxial capacitor.

3. The sample chamber was evacuated and filled with mercury Pressure was increased to slightly above atmospheric pressure. At the end of the low pressure phase the assembly was temporarily removed and re-weighed, then placed into the high pressure side of the apparatus.

4. Pressures were increased incrementally to a maximum of 55,000 psia.

5. Time was allowed for saturation equilibrium. The volume of mercury injected at each pressure was determined by the change in capacitance of the capillary stem.

6. The pressure was decreased to ambient and the sample unloaded. A final weight was recorded to calculate the residual mercury saturation.

7. Micromeritics data was imported to a spreadsheet and the mercury volumes and saturation were calculated. (Core Laboratories, 2012)

Samples B137 and B131 had a porosity fraction of 0.138 and 0.176 respectively. This porosity places them well within the average range for similar sandstones of 0.05-0.30. (Argonne National Laboratories, 2013) Pore throat size for B137 and B131 was 2.36 and 10.1 μm respectively. This classifies the sample as both having macroporosity which is also common with a sandstone. (Nelson, 2009) Permeability ranged from 33.8 mD to 372 mD for samples B137 and B131. This porosity places the samples higher than average for similar Ordovician sandstones, but accurately reflects the main contribution to reservoir permeability in the Central Michigan Basin. (Barnes et al, 1992)

Permeability and porosity are key Petrophysical factors affecting the reactivity of the injected CO_2. The Initial permeability and porosity of the sandstone needs to be sufficient to overcome possible damage caused by the injection. There may be a significant loss in core permeability between 35% and 55% after initial CO_2 injection due to the precipitation of reaction products as well as migration of clay particles through the formation. (Mohamed, 2012)

2.5 Experiments

Sample plugs were one inch in diameter and ranged from three to seven inches in length. From these parent plugs four reaction samples were cut and reacted with super critical CO_2 ($SCCO_2$) and synthetic brine inside a 20ml Parr reaction vessel. The plugs were then placed in the vessel and the storage environment reproduced using the $SCCO_2$ and a replicate of the native St. Peter brine. Observations were made over a period of 14 days.

During this time the pressure was maintained at a constant ~80bar/1160psi and temperature was maintained via a water/sand bath that was checked every 12 hours. The pressure inside the vessel needed to maintain the CO_2 in a liquid supercritical state was created by utilizing solid CO_2/dry ice. Because dry ice sublimates and expands to a consistent volume, the volume of dry ice needed to create the desired pressure of 80bar within the Parr reactor was determined using the van der Walls Equation of State (below), supplemented by input from Mr. Cristian Medina at the Indiana Geological Survey, who has substantial experience with pressurized reactions.

$$\left[P + a\left(\frac{n}{V}\right)^2\right]\left(\frac{V}{n} - b\right) = RT$$

	Sample 131	Sample 139	Sample 129	Sample 137
Wt. mg	2.64	2.689	2.673	2.648
CO_2 mg	4.5	4.5	4.5	4.5
Brine ml	2.1	2.3	2.1	2.2

Each sample was allowed to slowly warm to 70^{o}C in the water bath after sublimation of the CO_2 had occurred and pressure achieved. At the end of the 14-day period the canisters were removed from the bath and allowed to cool overnight. The reaction vessel was then slowly opened over a period of 24 hours to ensure a safe pressure decrease and to prevent any sudden change to the reacted samples.

RESULTS

Fabric Classification: Each plug was classified according to Folk's (1980) system to illustrate the sample composition as well as the diagenesis of the plugs used. Mineralogical analysis was done on the study samples to quantify possible compositional changes made to the sandstone as a result of the reaction with $SCCO_2$. Spectral analysis of the reaction brine showed that much of the reaction happened within the first 24 hours. There were not significant compositional changes shown in the XRD analysis.

3.1 Fabric Classification

The samples are sandstones, and classify as quartz arenites based on Folk's (1980) system. One of the four samples is well sorted (B–129), and the other three have bimodal sorting characteristics (B–131, B-137, B-139). All samples exhibit a massive fabric, containing sub rounded to rounded grains. Point grain contacts typify the samples, providing evidence of light compaction. Grain sizes range from upper fine sand to coarse sand size. This range of grain sizes is evident in the bimodally sorted samples. The bulk of the framework grains are monocrystalline quartz (x to y percent, Table XYZ). Present in lesser amounts are K–feldspar grains (X to y percent, Table XYZ). The feldspar grains tend to be significantly smaller than the quartz grains and are more angular. Micas and heavy minerals are also present in trace to minor amounts. In sample B–129, quartz overgrowths are the primary cement. There is a significant presence of illite/chlorite clay in the grain interstices (indicating it is an early diagenetic product) which is not present in areas near quartz overgrowths. The degree and volume of

cementation is not significant in any of the samples, thereby yielding abundant primary intergranular pores. In a few places, leaching of unstable feldspar produces a few secondary intra-angular pores.

3.2. Mineralogical Analysis

3.2.1. Spectral Analysis

Analysis of the brine during the reaction of sample B137 and B129 showed that a significant portion of the total geochemical reaction occurred within the first 24 hours of the process with the reaction being essentially finished within the first 3 days. Analysis of the brine tracked the geochemical changes caused by the interaction of the super critical CO_2 with the brine and sandstone sample. Figure 11a-g show concentrations of the measured elements over the course of the two week reaction time.

3.2.2 X-Ray Diffraction Analysis

XRD diffractograms showing a 2θ range from 10^o to 80^o confirm that each of the samples is quartz arenite and there was no significant change in bulk composition as a result of reaction with super critical CO_2. The secondary heavy minerals and potassium feldspar observed from petrographic analysis did not appear on the XRD scans of the pre- or post-reaction samples. Samples B129 and B139 did show possible calcite development but these spikes were not consistent when compared with each other. Sample B131 and B137 did not show similar spikes in the 29^o to 36^o 2θ. The XRD diffractograms are included in the appendix.

DISCUSSION

Petrographic, x and y analysis indicate that samples of The St. Peter Formation examined are comprised primarily of mature quartz arenite with a porosity range of approximately 15-20%. In the Illinois basin the St. Peter Formation is submerged in a regional salt water brine (Leetaru et al, 2005; Pitman et al, 1997) and in the basin the St. Peter is at a depth and pressure that enables the storage of waste CO_2 in a liquefied, super critical state (Barnes et al, 1992; Pitman et al, 1997; Nordbotten et al, 2005). CO_2 becomes super critical at 31.1°C and 73.8 bar (Jessop & Leitner, 1999). Other regionally contiguous sandstone formations with this combination of porosity and permeability, as well as depth and pressure of the formation within the brine has been targeted in other works as potential long term storage sites for waste CO_2 (Ambrose et al, 2006; Doughty et al, 2001; Liu et al, 2011).

These samples used in this study follow the overall compositional trend of the formation, but show typical localized variations in grain size, cement percentage, porosity and permeability. Additional analyses of the St. Peter verify the overall homogeneity but regional variations (Hoholick, 1980; Hoholick and Metarko, 1984; Pitman et al, 1997; Girard and Barnes, 1995)

These variations could be a result of localized deformation, changes in the matrix porosity and possible fractures in the formation itself or the overlying cap rock. The ensuing structural variety influences overall flow permeability and consequently the flow field. (Tsang et al, 2006). These factors combined can lead to local heterogeneity within the larger homogeneous body of the formation (Mathis and Sears, 1984) which

complicates CO_2 injection site selection and viability and justify individual mineralogical assessment of multiple injection sites when considering the injection potential of the formation as a whole (Solomon, 2007).

In each of the samples there was a significant increase in porosity after reaction with super critical CO_2. Samples B131, B137 and B139 saw an increase in porosity of 49.92%, 48.60% and 121.56% respectively. Similar increase in porosity after $SCCO_2$ injection have been observed in multiple studies (Izgec et al, 2008; Liu et al, 2011). This increase in porosity and permeability can be attributed to not only geochemical processes, but also mechanical processes, especially deformation and fracturing due to increased pressure at the injection site (Tsang et al, 2006). Although there has been evidence of decreased porosity in bedded sandstone after CO_2 injection. This was attributed to carbonate precipitation resulting from mass leaching of nearby shales (Xu, 2004). Sample B129 disintegrated in each of four reactions and post reaction porosity could not be obtained. This level if increase in porosity is significant, but substantial increases in porosity from $SCCO_2$ injection are found in other works (Rosenbauer, 2005; Eggerman, 2006; Adebayo, 2013).

The observed post-treatment increase in porosity was primarily due to the dissolution of the intragranular feldspar and clay minerals. Similar dissolution has also been shown in $SCCO_2$ injection projects involving sandstone. (Leone, 1988; Gaus, 2009) This dissolution in turn allowed quartz crystals to break free from the sample piece. Sample B129 consistently crumbled each time when reaction with $SCCO_2$ was attempted, however it's worth noting that this crumbling may have occurred in a two-

stage process. When the reaction vessel was depressurized quickly in the brine reaction experiment at Washington University the plug was only broken into a few large chunks, but broke down into individual grains within 5 minutes. Also, the B129 plug used at the Washington University location was exposed to iron leaching from the reaction vessel. This iron coated the sample giving it an orange hue on the outside. As a result the chunks seen on the sample before the final breakdown had iron coated surfaces and fresh surfaces that seemed to have occurred very recently, showing the sample was likely intact before depressurization. It is possible that moving the sandstone plug B129 into the high pressure environment of the test rig could have weakened the matrix and increased the porosity on a microscopic level within the sample (Takahashi, 2005). After depressurization the sample crumbled due to the weakened structural matrix.

Sample B131, B137 and B139 did maintain their form after reaction, but were noticeably softer and each of those plugs were smaller as a result of the outer layer of grains being washed into the brine. Post reaction permeability change as a result of reaction with $SCCO_2$ could not be estimated effectively from porosity. This is due to the fact that there was very little correlation between porosity and permeability in the pre-reacted samples. Permeability varied in other studies as well (Ricardo, 2012; Adebayo, 2013). Petrographic analysis and XRD did not show definitive change in mineralogical composition as a result of the $SCCO_2$ injection. However ICP-MS analysis of the brine did show evidence of dissolution as noted in figures 12a-12g. Similar results were seen over a longer period (Rosenbauer, 2005). XRD analysis did show some secondary mineral

development in the form of calcium carbonate, but this was inconclusive between samples.

As the CO_2 dissolved into the brine it formed carbonic acid. This carbonic acid reacted with the potassium feldspar to form kaolinite secondary clays that entered the brine solution and were washed out of the matrix:

$$CO_2\ (aq) + H_2O \ll H_2CO_3\ (aq)$$

$$4KAlSi_3O_8 + 4H_2CO_3 + 2H_2O \rightarrow Al_4Si_4O_{10}(OH)_8 + 4K+ + 4HCO_3- + 8SiO_2$$

This transition from potassium feldspar to the kaolinite clay is seen in the brine reaction figure 3.2.1a and 3.2.1d. This has been seen in other CO_2 injection projects involving sensitive smectite clays dispersing kaolinite. (Leone et al, 1988) These data show an initial spike in potassium and aluminum as these elements are dissolved into the brine when the feldspar is reacted (Rosenbauer, 2005). Potassium and aluminum levels drop as the potassium feldspar precipitates and secondary clays are developed over the remainder of the two week reaction. Petrographic analysis showed that the increase in intragranular pore space offered an increase in porosity in samples B131, B137, and B139.

The results discussed here are best categorized in the body of works involving injection site reactions. It is likely that the dramatic increase in porosity seen in the samples can be attributed to the abundance of $SCCO_2$ compared to the defined volume of brine and rock studied. Near well bore increases in porosity have been seen in other works (Xu, 1999; Essendelft, 2005). Modeling the possible fluid flow within the reservoir

over time could give a better idea of the long-term storage mechanics. (Nordbotten et al, 2005)

Further work in this area should involve a greater number of samples analyzed at different time intervals with distinct differences in pressure, $SCCO_2$ concentration and sample size since it has been established that variation in porosity, permeability and overall rock/water/CO_2 interaction change significantly the greater distance you are from the injection site (Bertier et al, 2005).

Post reaction mercury injection porosity as well as post reaction permeability analysis would better define the holistic impact of $SCCO_2$ injection. Computer modeling of the CO_2 plume using sample porosity, permeability, temperature and pressure could be used to determine impact on the porosity and permeability of the St. Peter sandstone over a larger geographic area, which is vital to establishing the long term storage capacities of the selected injection site (Gaus, 2002; Essendelft, 2005) This in turn could give better insight regarding the true storage capacity of the formation.

CONCLUSION

The viability of the St. Peter Sandstone as a long term storage reservoir for CO_2 depends not only on its location in the subsurface, but also the primary fabric of formation in combination with the reactivity of the sandstone with CO_2 rich brine. Injecting $SCCO_2$ into the St. Peter Formation may increase porosity and permeability through dissolution of the k-feldspar and clays. This affords an increase in initial storage capacity possibly leading to more effective long term storage in the form of mineral trapping via precipitation as calcite, magnesite and other minerals.

The preliminary research presented here illustrates that the portion of the St. Peter located in the portion of the Illinois Basin in Southern Illinois may make a viable storage site for waste CO_2 from power plants in the region. The St. Peter depth in this region affords the needed temperature and pressure to maintain the injected CO_2 in the liquid super critical state. There are also sufficient cap layers to inhibit upward migration into surface or near surface ground water. Finally the petrological and geochemical properties of the formation lends itself well to CO_2 storage by affording increased porosity and permeability after reaction with injected CO_2.

While this research has been preliminary, it does show that further investigation into the storage capacity of the St. Peter Sandstone is warranted. Obtaining and testing a larger number of core samples from the St. Peter within the deeper portion of the Illinois Basin could offer a better understanding of porosity and permeability within the St. Peter in the region where it potentially will be used as a storage reservoir. In addition, a longer reaction time with a greater number of samples could reveal subtle,

secondary reactions that were not readily apparent in this data. All this combined will give a better understanding of the suitability of the St. Peter for CO_2 storage and possibly warrant a test injection site in future studies.

FIGURES

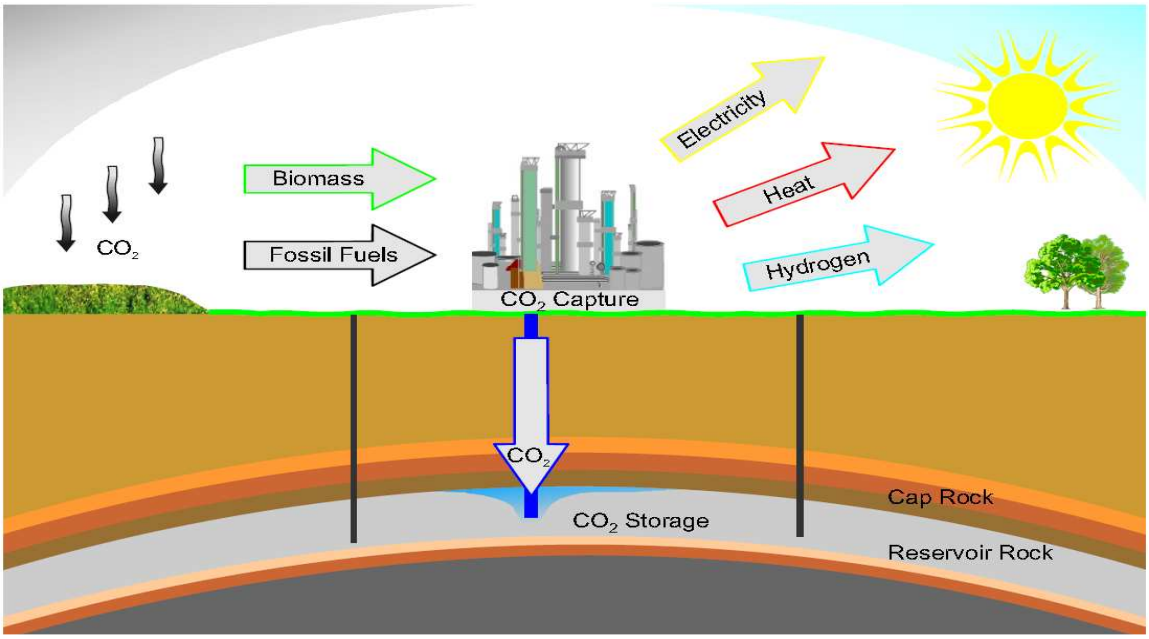

Fig 1: Geologic CO_2 Capture (CO_2 Sink flyer, 2012)

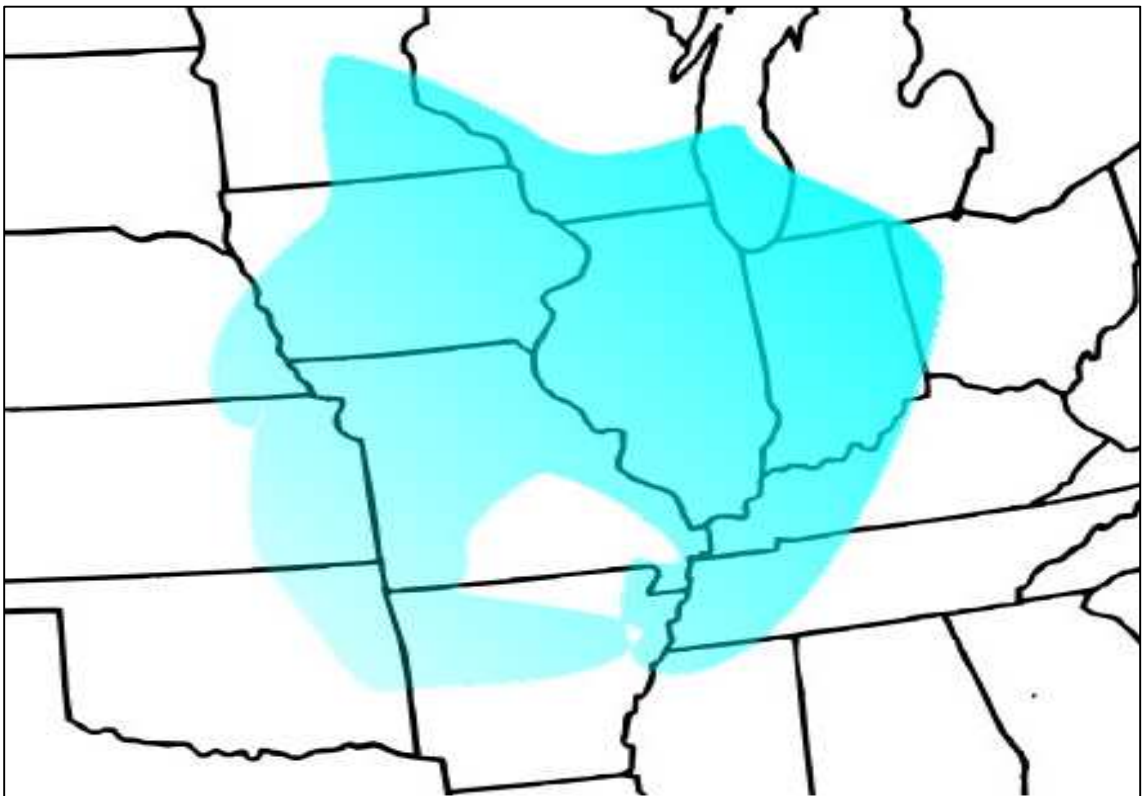

Fig 2: Coverage of the St. Peter Sandstone in the U.S.

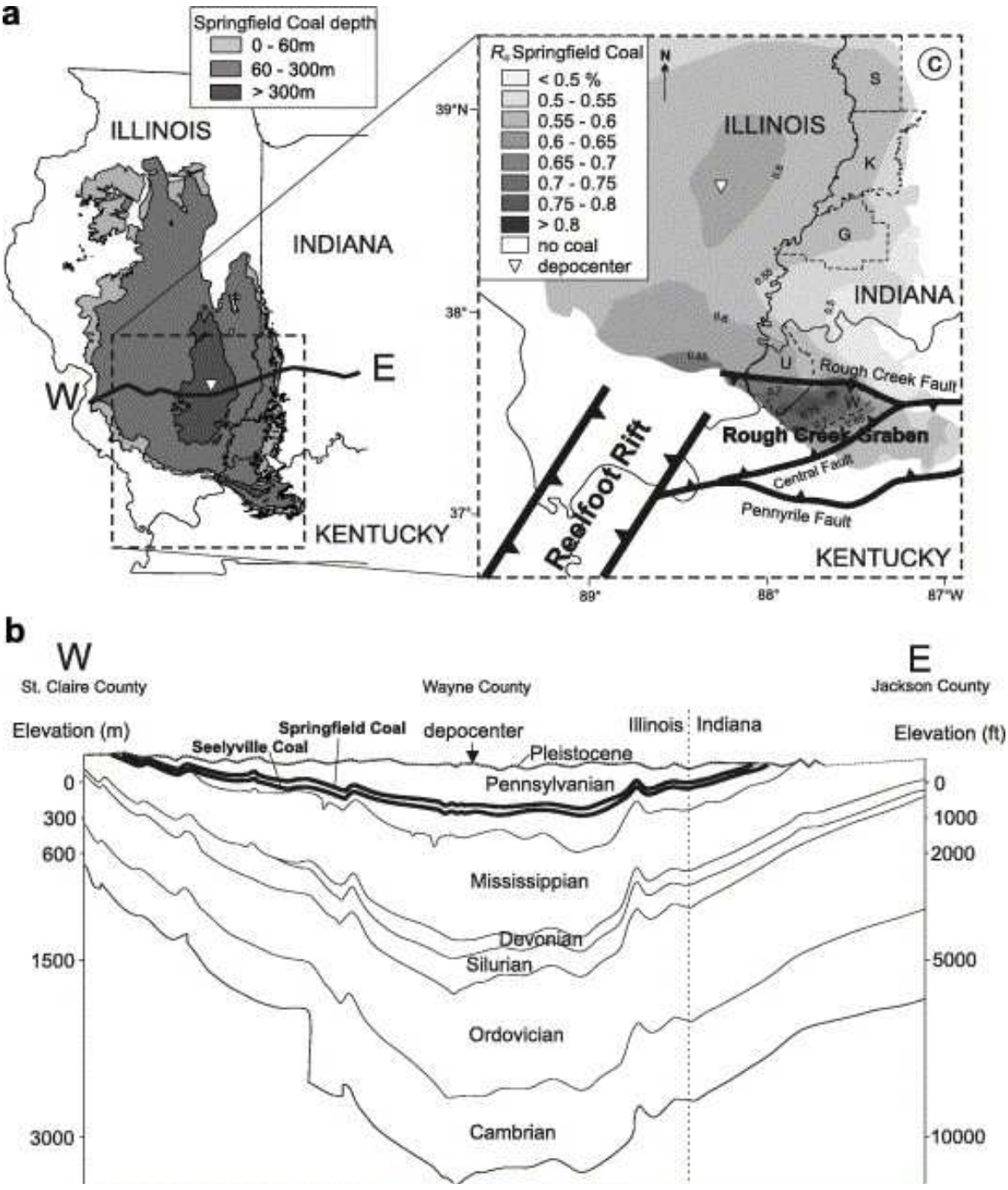

Fig 3: Cross section of the Illinois Basin (Strąpoć, 2007)

Fig. 4: County map of Indiana highlighting Fulton and Starke County.

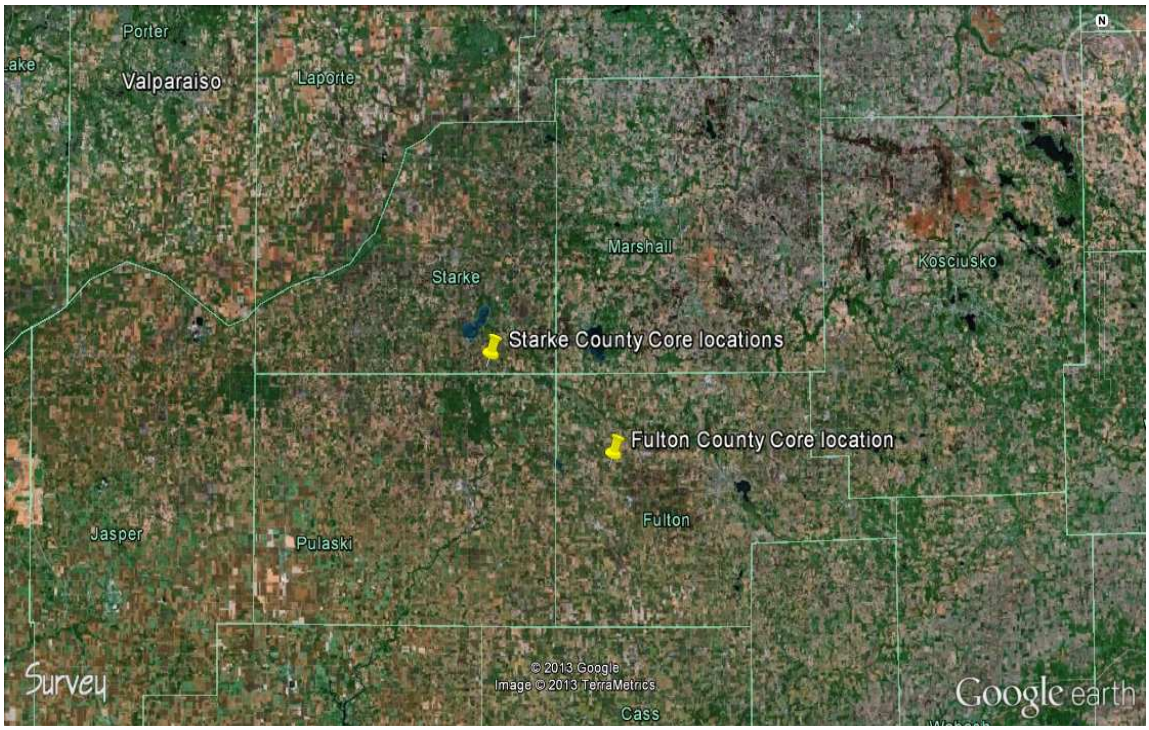

Fig. 5: Well locations. Sample B131 and B129 are from the Starke County site and sample B139 and B137 are from the Fulton County site.

Sample B129 St. Peter Sandstone
Fulton County Indiana
Depth 444.5 meters
IGS Core Box# 1458.5-1459.8
Pre-reaction porosity 19.92%
Pre-reaction permeability 215 md
Grain density 2.658 g/cm^3

Sample B131 St. Peter Sandstone
Fulton County Indiana
Depth 450.1 meters
IGS Core Box# 1475.8-1476.6
Pre-reaction porosity 18.75%
Pre-reaction permeability 981 md
Grain density 2.640 g/cm^3

Sample B137 St. Peter Sandstone
Stark County Indiana
Depth 434.2 meters
IGS Core Box# 1424.5-1425.0
Pre-reaction porosity 16.44%
Pre-reaction permeability 34.1 md
Grain density 2.644 g/cm^3

Sample B139 St. Peter Sandstone
Stark County Indiana
Depth 439.4 meters
IGS Core Box# 1441.5-1442.1
Pre-reaction porosity 15.72%
Pre-reaction permeability 26.0 md
Grain density 2.689 g/cm^3

Fig. 6: Sample fabric illustration.

Sample B129 thin section / pre-reaction / 40X magnification

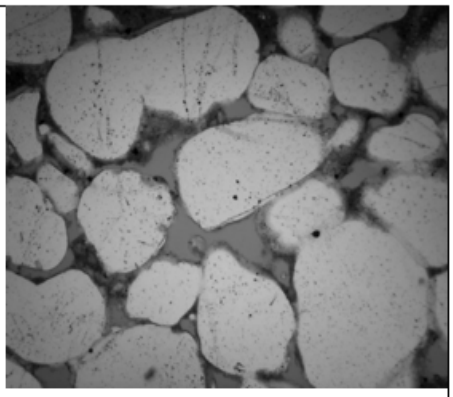

Structure: Well sorted; light to moderate compaction; sub-rounded to rounded grains.

Framework Grains: Abundant monocrystalline quartz; trace K-feldspar.

Cement: Minor to moderate quartz overgrowths; trace feldspar overgrowths; some illitic and chloritic clay.

Pore Type: Abundant primary intergranular pores; trace moldic pores; rare secondary intragranular pores.

This sample is a sandstone contained well sorted, sub-rounded to rounded framework grains with light to moderate compaction. There is sporadic intergranular clay that appears to be a mixture of illite and chlorite. A few K-feldspar grains are also apparent in the photomicrographs. Early diagenetic illite/chlorite and infiltrated detrital clay distribute between framework grain contacts, indicating that the clay formed or was emplaced before mechanical compaction and quartz overgrowths. The light cementation in this sample leaves abundant intergranular pore space.

Sample B131 thin section / pre-reaction / 40X magnification

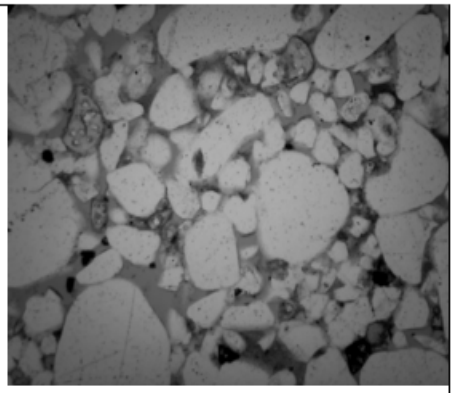

Structure: Bimodal sorting; light to moderate compaction; sub-rounded grains.

Framework Grains: Abundant monocrystalline quartz; minor K-feldspar.

Cement: Minor to moderate quartz overgrowths; some illitic and chloritic clay.

Pore Type: Abundant primary intergranular pores; trace moldic pores; rare secondary intragranular pores

The sample exhibits bimodal sorting. Two size classes are evident: coarse sand and upper fine sand. The coarse fraction only contains monocrystalline quartz grains and the upper fine sand-size fraction contains quartz, trace k-feldspar and heavy minerals. Quartz overgrowths are a trace cement in this sample. Illite/chlorite appear between framework grains, indicating the clays infiltrated or formed early in the sample's diagenetic history. The quantity of the intergranular clays is not high, and combined with the open fabric of the sample, yields abundant primary intergranular pores and a few secondary intragranular pores resulting from feldspar leaching.

Fig. 7: Sample structure, framework, cement and pore type.

Sample B137 thin section / pre-reaction / 40X magnification

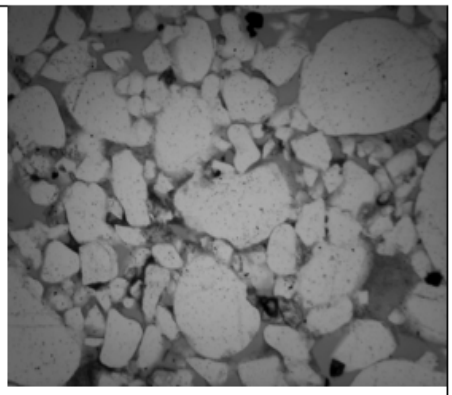

Structure: Bimodal sorting; light to moderate compaction; sub -rounded to rounded grains.

Framework Grains: Abundant monocrystalline quartz; minor K-feldspar.

Cement: Minor to moderate quartz overgrowths; some illitic and chloritic clay.

Pore Type: Abundant primary intergranular pores; trace moldic pores; rare secondary intragranular pores

The sample exhibits bimodal sorting. Two size classes are evident: coarse sand and upper fine sand. The coarse fraction only contains monocrystalline quartz grains and the upper fine sand-size fraction contains quartz, K-feldspar and heavy minerals. The smaller framework grains are not as well rounded as the larger grains. Quartz overgrowths are a trace cement in this sample. Illite/chlorite appear between framework grains, indicating the clays infiltrated or formed early in the sample's diagenetic history. The quantity of the intergranular clays is not high in this sample, and combined with the open fabric of the sample, yields abundant primary intergranular pores and a few secondary intragranular pores resulting from feldspar leaching.

Sample B139 thin section / pre-reaction / 40X magnification

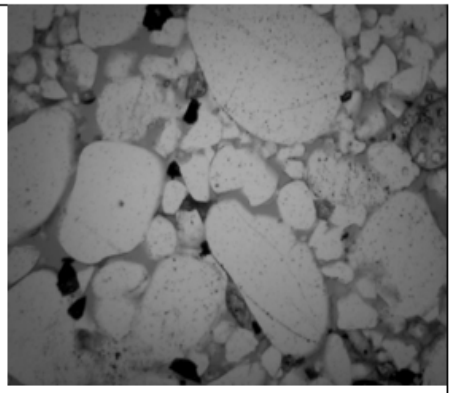

Structure: Bimodal sorting; light to moderate compaction; sub -rounded grains to rounded grains.

Framework Grains: Abundant monocrystalline quartz; minor K-feldspar.

Cement: Minor to moderate quartz overgrowths; some illitic and chloritic clay.

Pore Type: Abundant primary intergranular pores; trace moldic pores; rare secondary intragranular pores.

The sample exhibits bimodal sorting. Two size classes are evident: coarse sand and upper fine sand. The coarse fraction only contains monocrystalline quartz grains and the upper fine sand-size fraction contains quartz, trace k-feldspar and heavy minerals. The smaller framework grains are not as well rounded as the larger grains. Quartz overgrowths are a trace cement in this sample. Illite/chlorite appear between framework grains, indicating the clays infiltrated or formed early in the sample's diagenetic history. The quantity of the intergranular clays is not high, and yields abundant primary intergranular pores and a few secondary intragranular pores from feldspar leaching.

Fig. 7: Structure, framework, cement and pore type (continued).

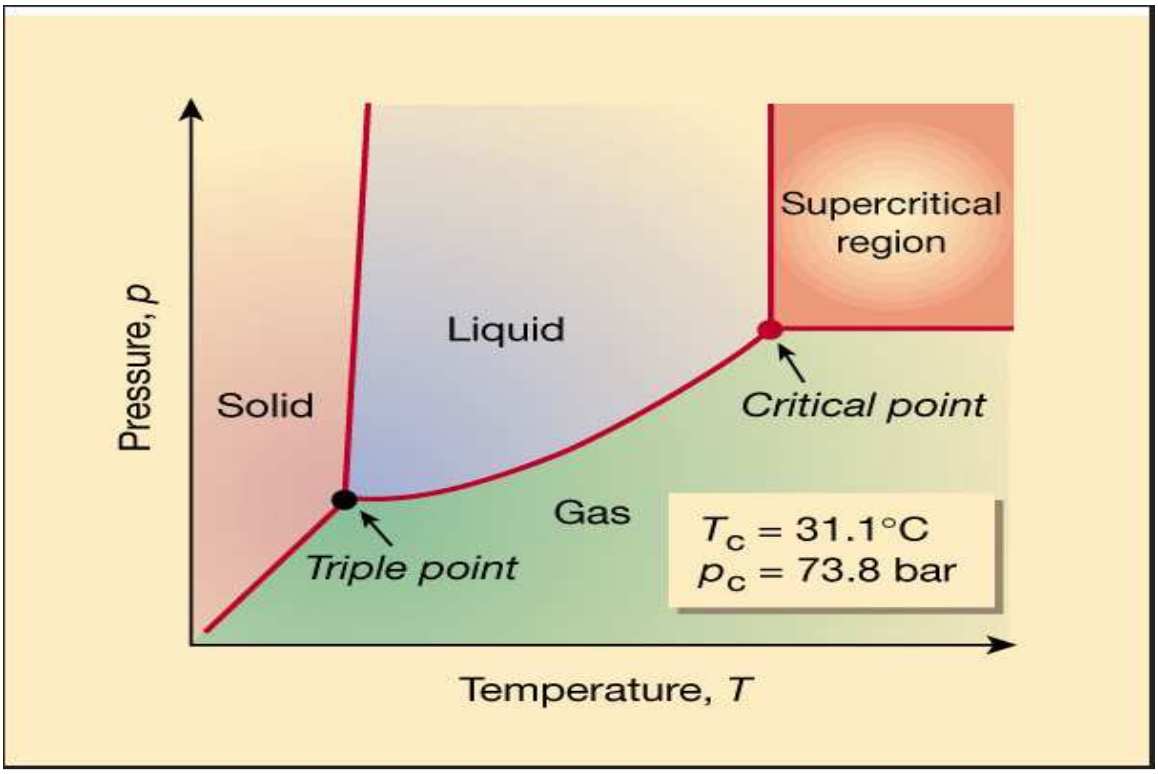

Fig. 8: Phase relationship of CO_2 (Jessop & Leitner, 1999)

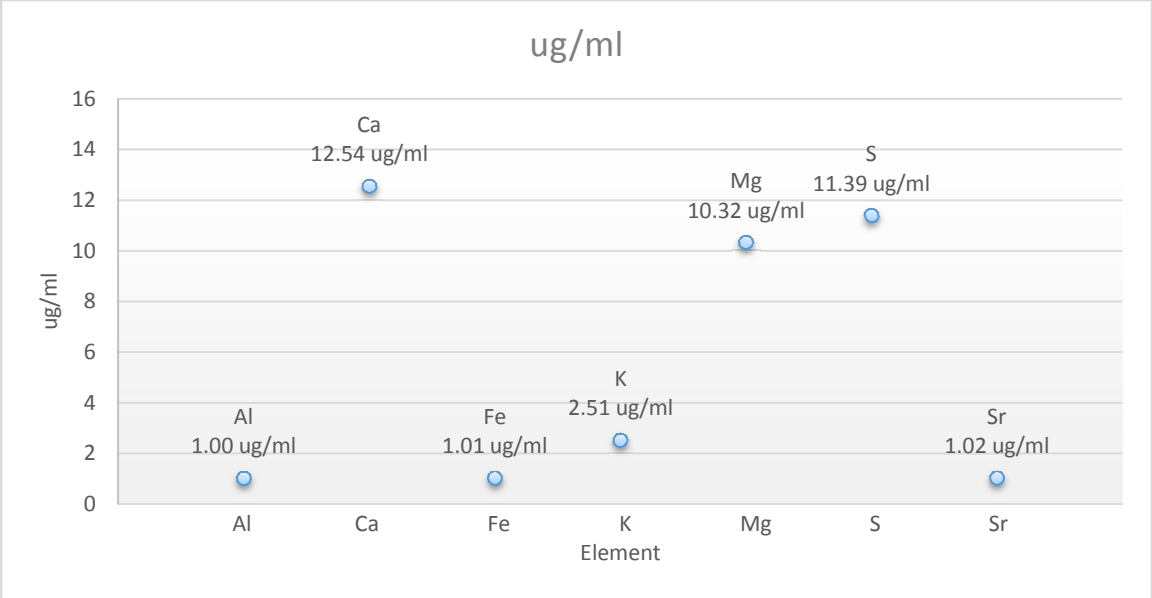

Fig. 9: Initial elemental composition of the St. Peter Brine.

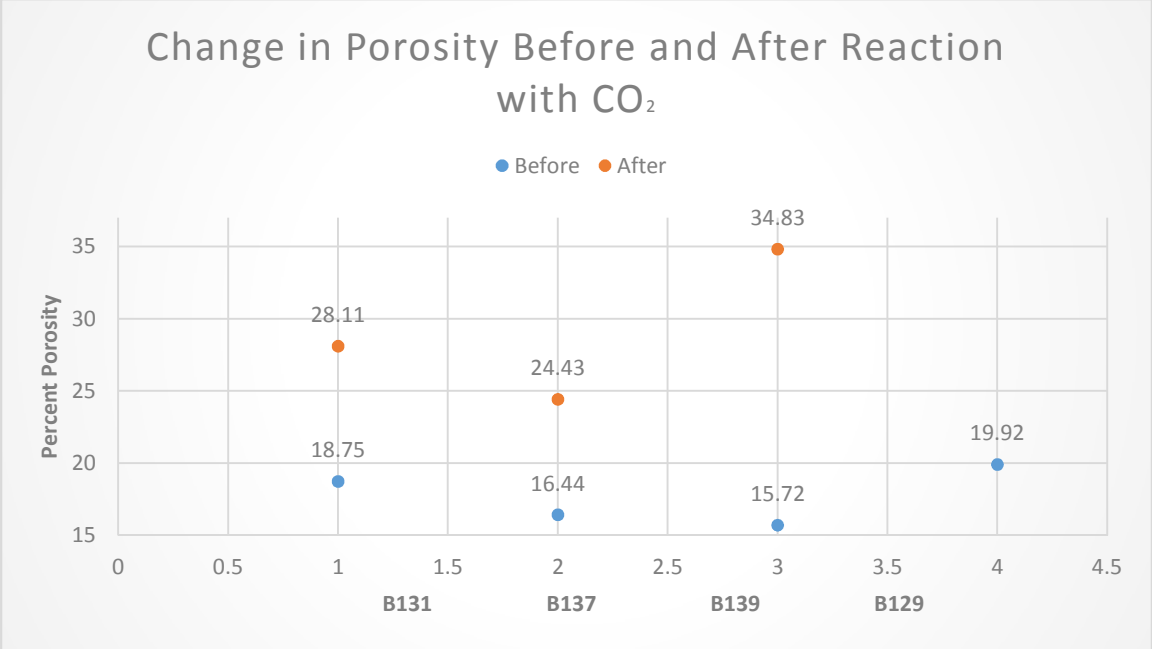

Fig. 10: Change in porosity for samples B131, B137, and B139 as a result of reaction with supercritical CO_2.

Sample B131 thin section / post-reaction / 40X magnification

Framework Change: The monocrystalline quartz remains, but the K-feldspar was significantly reduced.

Cement Change: Quartz overgrowths remain, clay was reduced.

Pore Type: Primary intergranular pores.

The sample still exhibits bimodal sorting consisting of coarse sand and upper fine sand. The coarse fraction contains monocrystalline quartz grains and the upper fine sand-size fraction still contains quartz and heavy minerals, but the k-feldspar is significantly reduced.

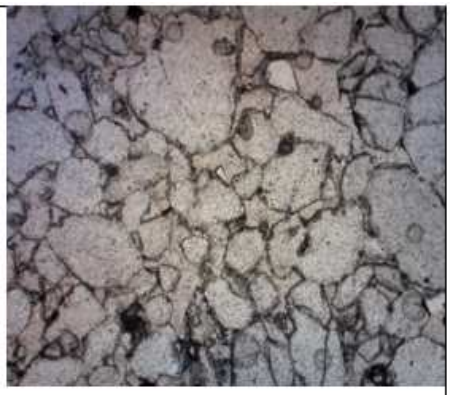

Sample B137 thin section / post-reaction / 40X magnification

Framework Change: The monocrystalline quartz remains, but the K-feldspar was significantly reduced.

Cement Change: Quartz overgrowths remain, clay was reduced.

Pore Type: Primary intergranular pores.

Bimodal sorting of the quartz grains remains as does the heavy minerals. K-feldspar is noticeably absent. The Quartz overgrowths are the primary cement in this sample.

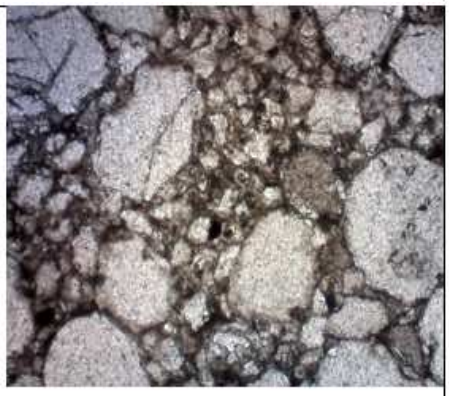

Sample B139 thin section / post-reaction / 40X magnification

Framework Change: The monocrystalline quartz remains, but the K-feldspar was significantly reduced. Heavy minerals remain.

Cement Change: Quartz overgrowths remain, clay was reduced.

Pore Type: Primary intergranular pores.

The bimodal sorting remains consisting of coarse sand and upper fine sand. The coarse fraction contains monocrystalline quartz grains and the upper fine sand-size fraction contains quartz and heavy minerals. The k-feldspar is absent in most images. Quartz overgrowths are the cement in this sample.

Fig. 11: Post-reaction thin section images of samples B131, B137 and B139. Quartz crystals and heavy minerals remain but the k-feldspar and clays found in the pre-reaction samples are significantly reduced.

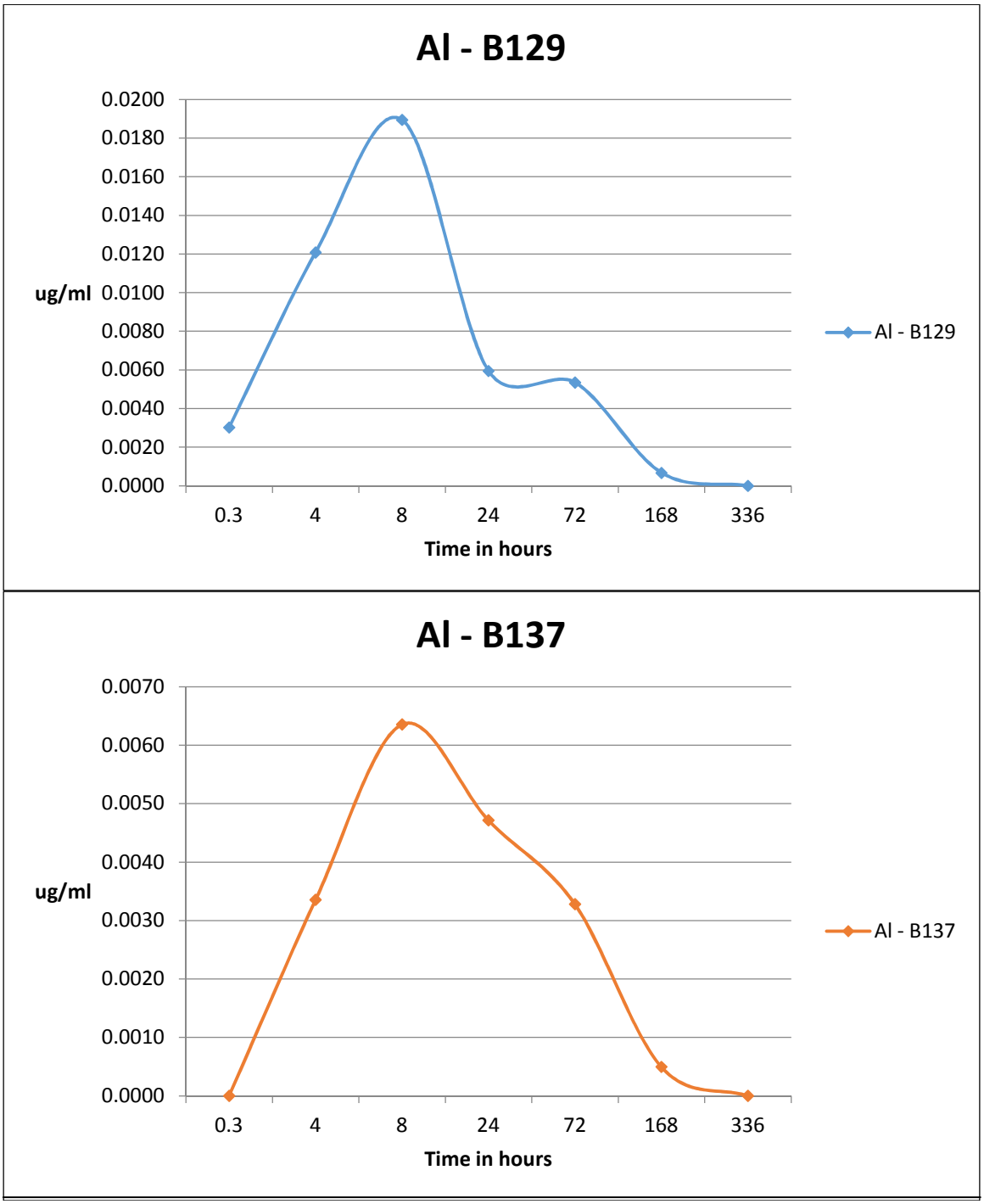

Fig. 12a: Aluminum spiked in both samples shortly after the reaction began and then slowly normalized over the following two week period.

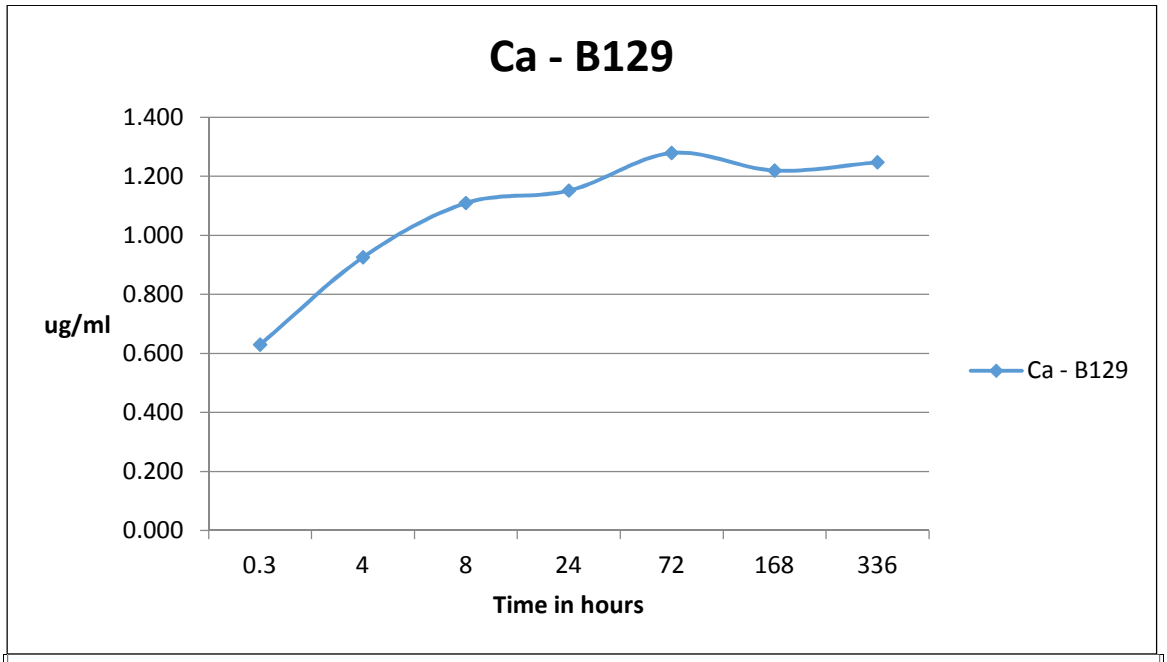

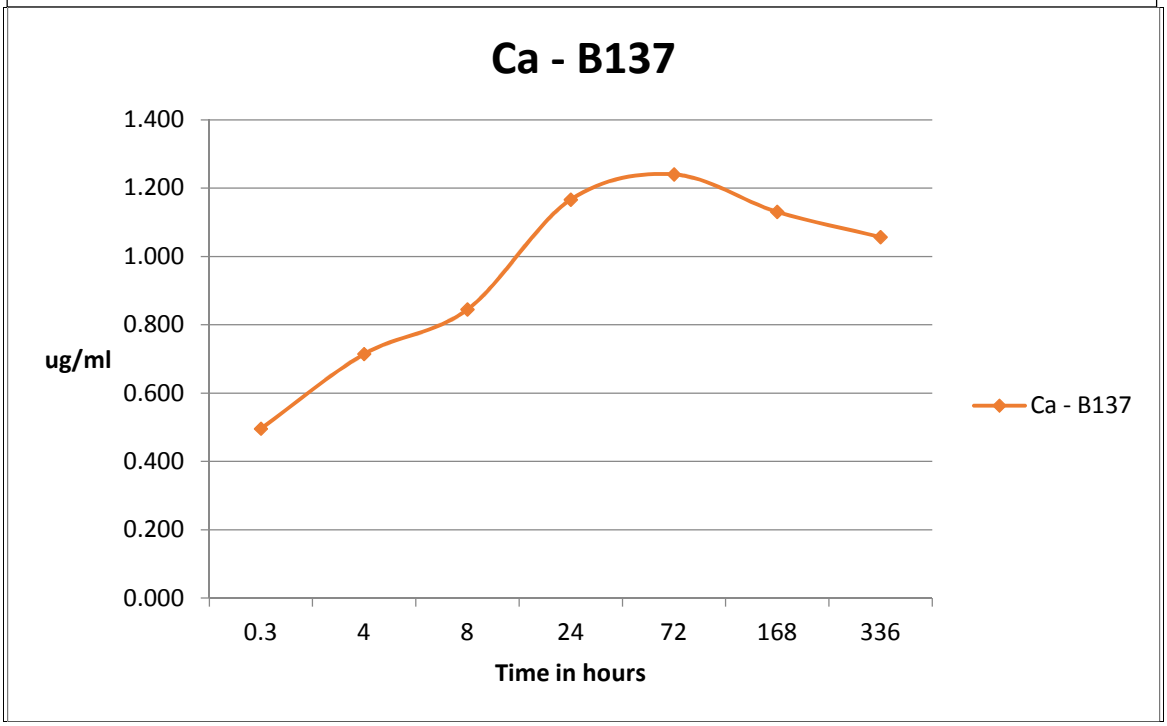

Fig. 12b: Calcium rose over the first 24 hours and remained relatively stable over the remaining two week period.

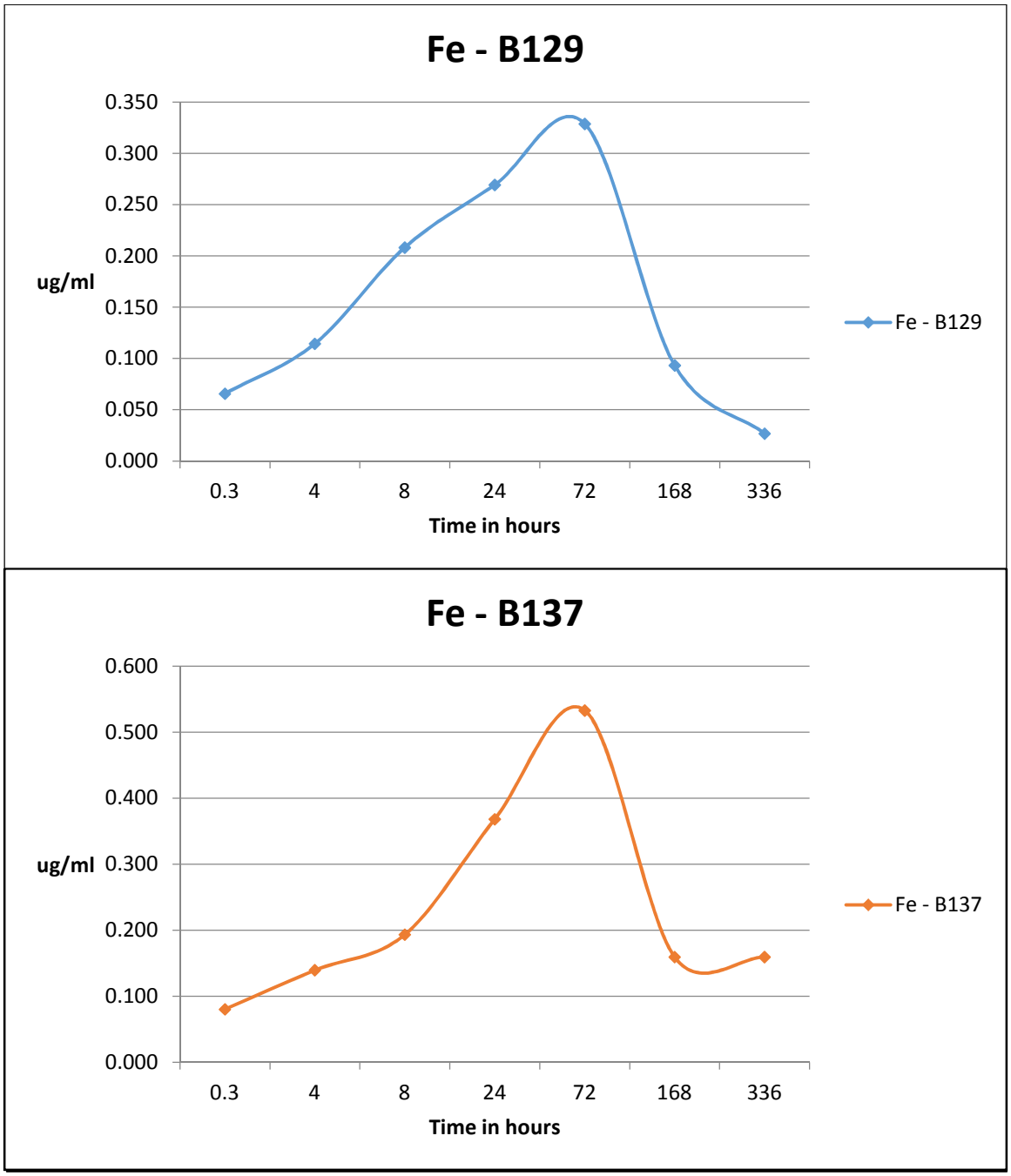

Fig. 12c: Iron peaked shortly before the three day mark, then dropped off slowly over the next 3 days – remaining stable for the final week of the reaction.

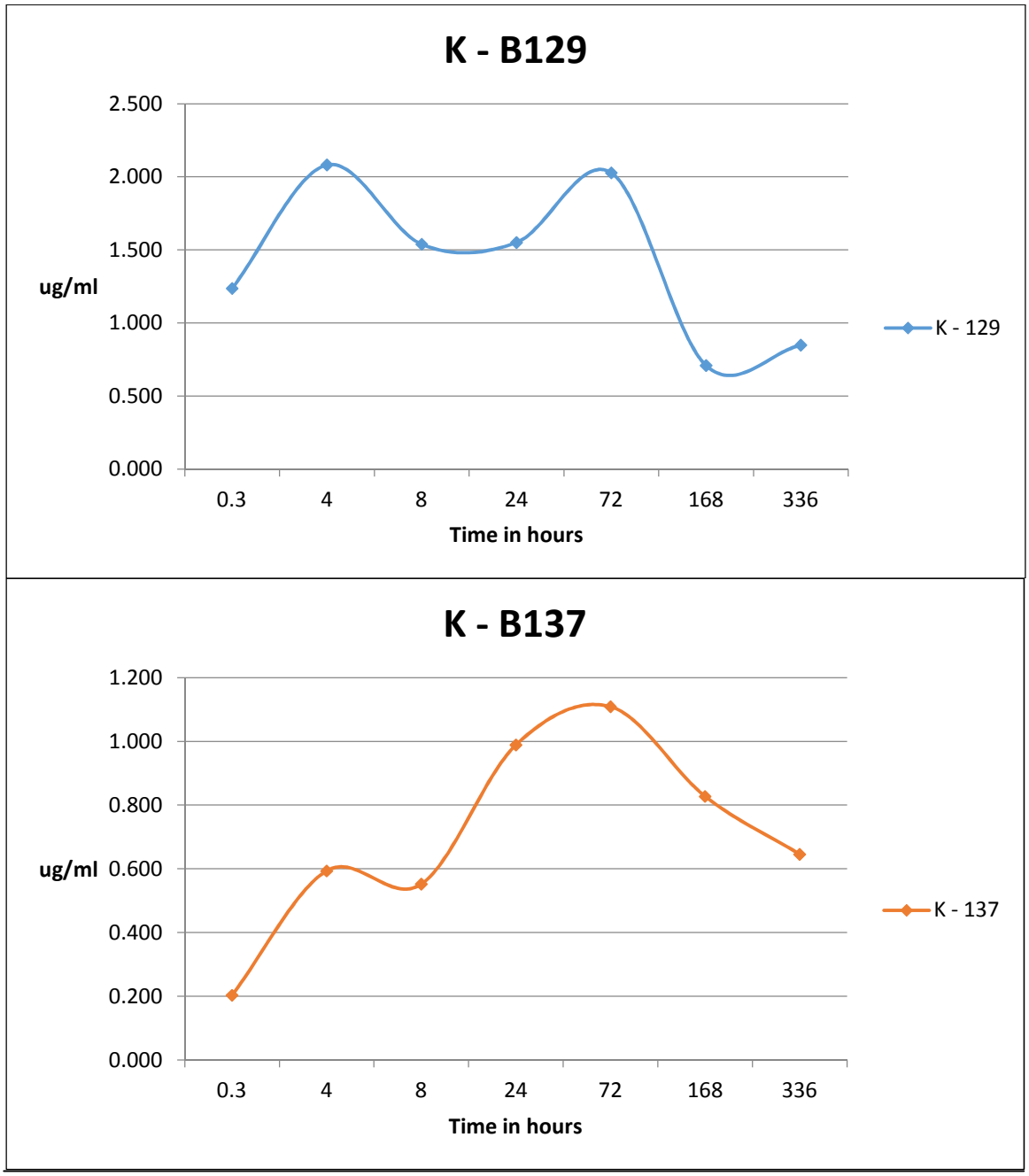

Fig. 12d: Potassium levels varied between the two tested samples. Consistencies are an initial spike then dip in the early hours with a gradual rise over the first 48 hours and a gradual drop off over the remaining 11-12 days.

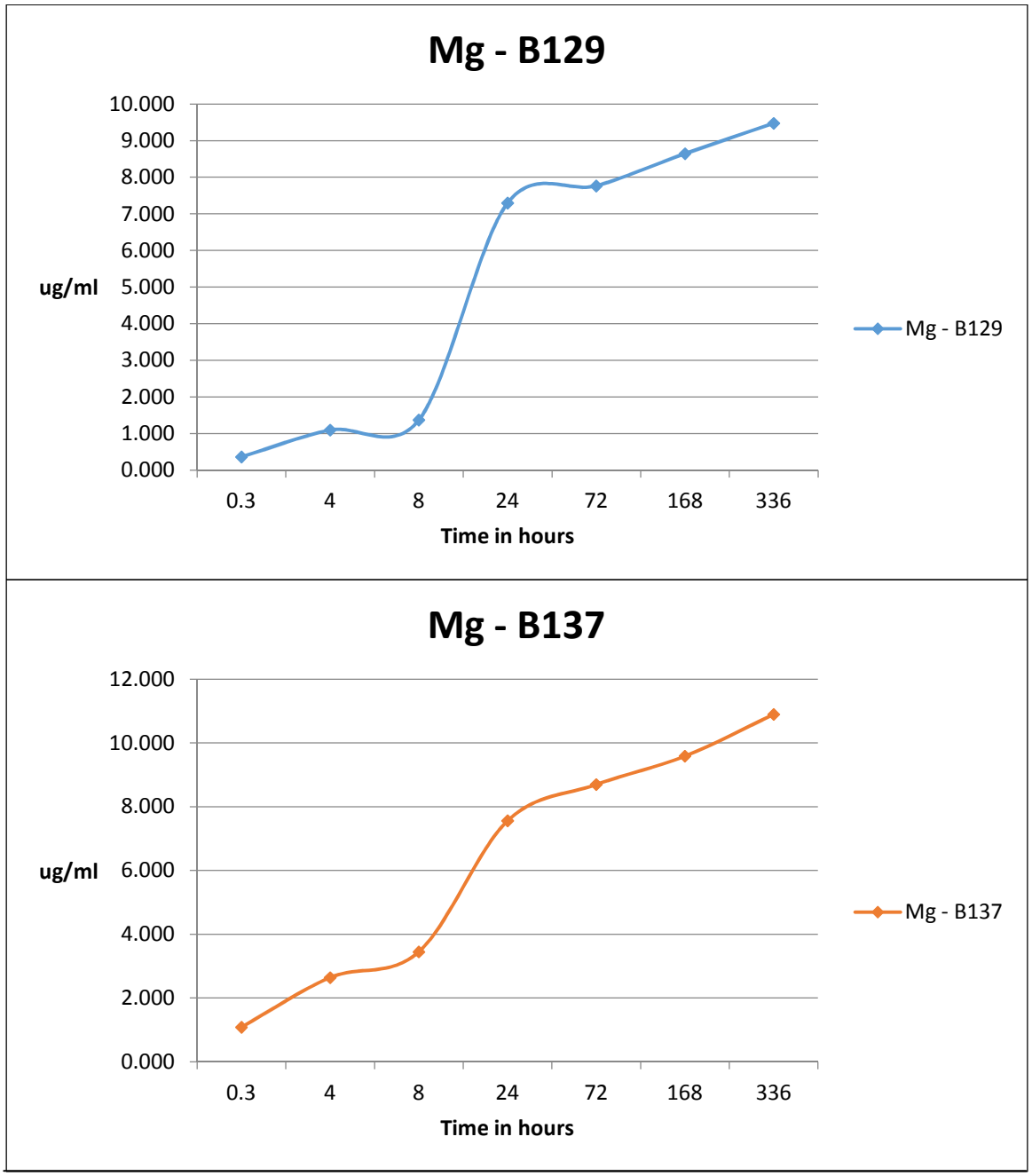

Fig. 12e: Magnesium levels rose consistently over the first 48 hours in both samples, then shifted to a more gradual rise over the next 12 days.

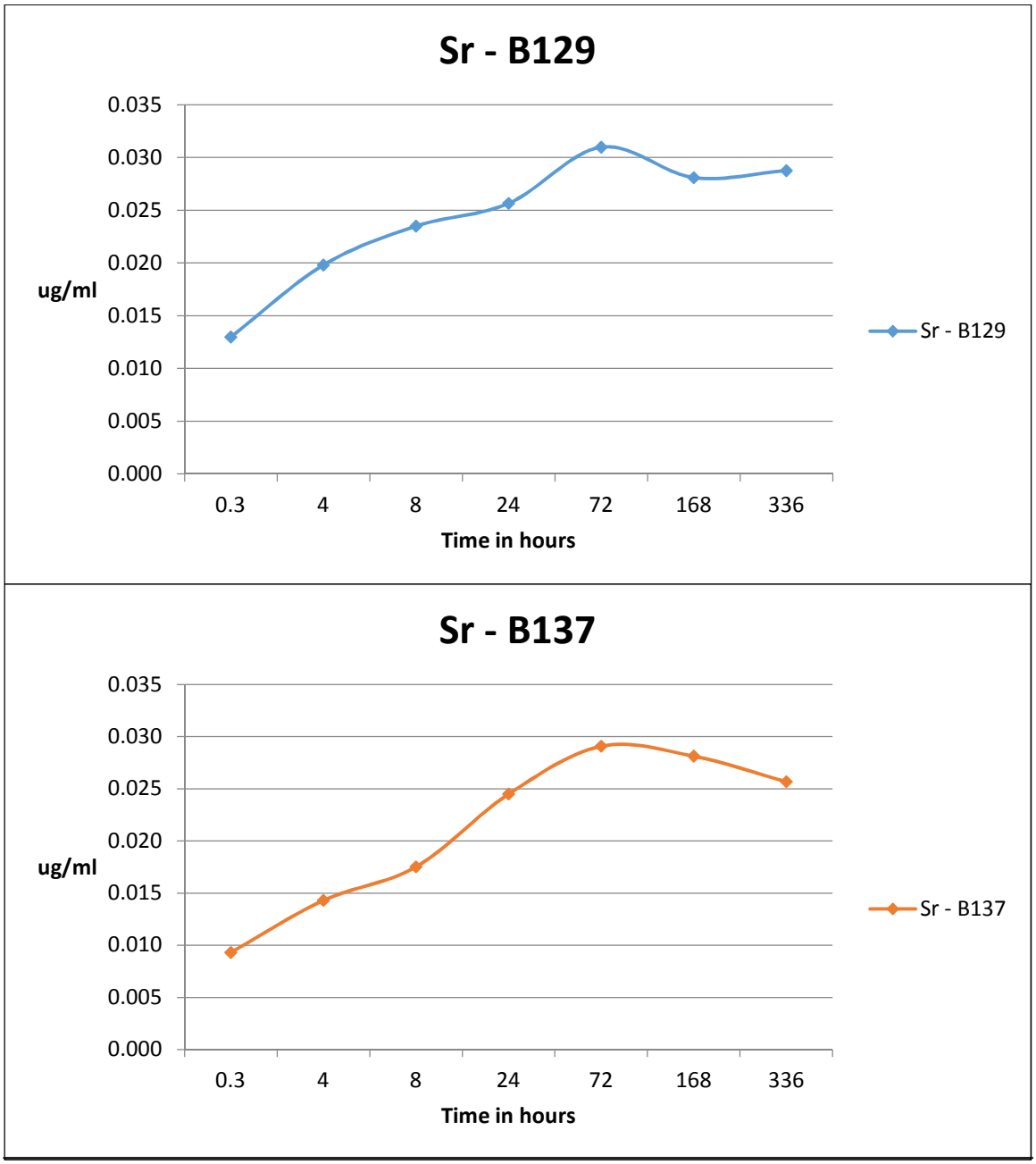

Fig. 12f: Strontium levels rose consistently over the first 48 hours, then slowed and began to decline after 3 days.

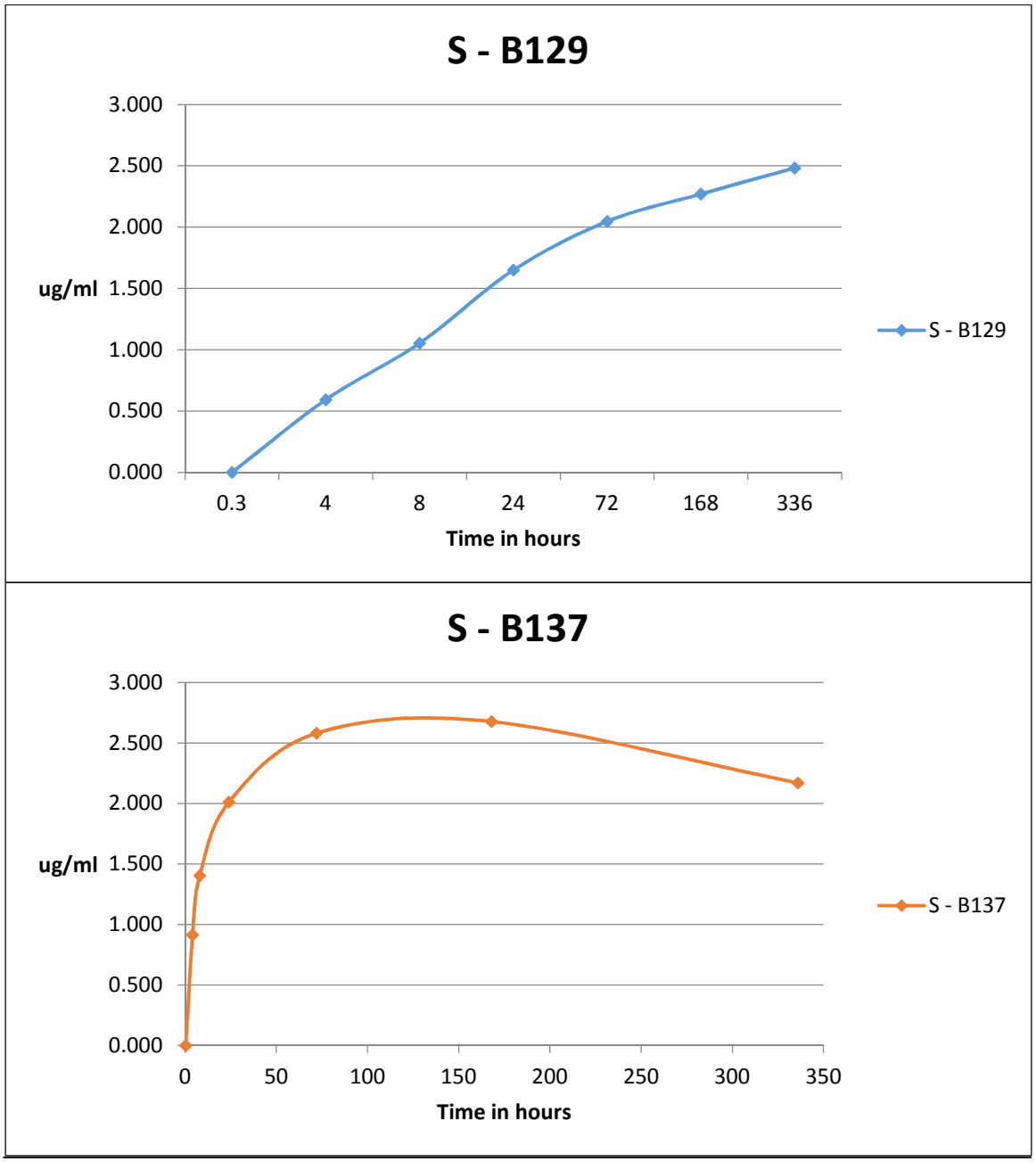

Fig. 12g: Sulfur levels dropped almost immediately as the brine came in contact with the super critical CO_2 and then gradually rose to pre-injection levels.

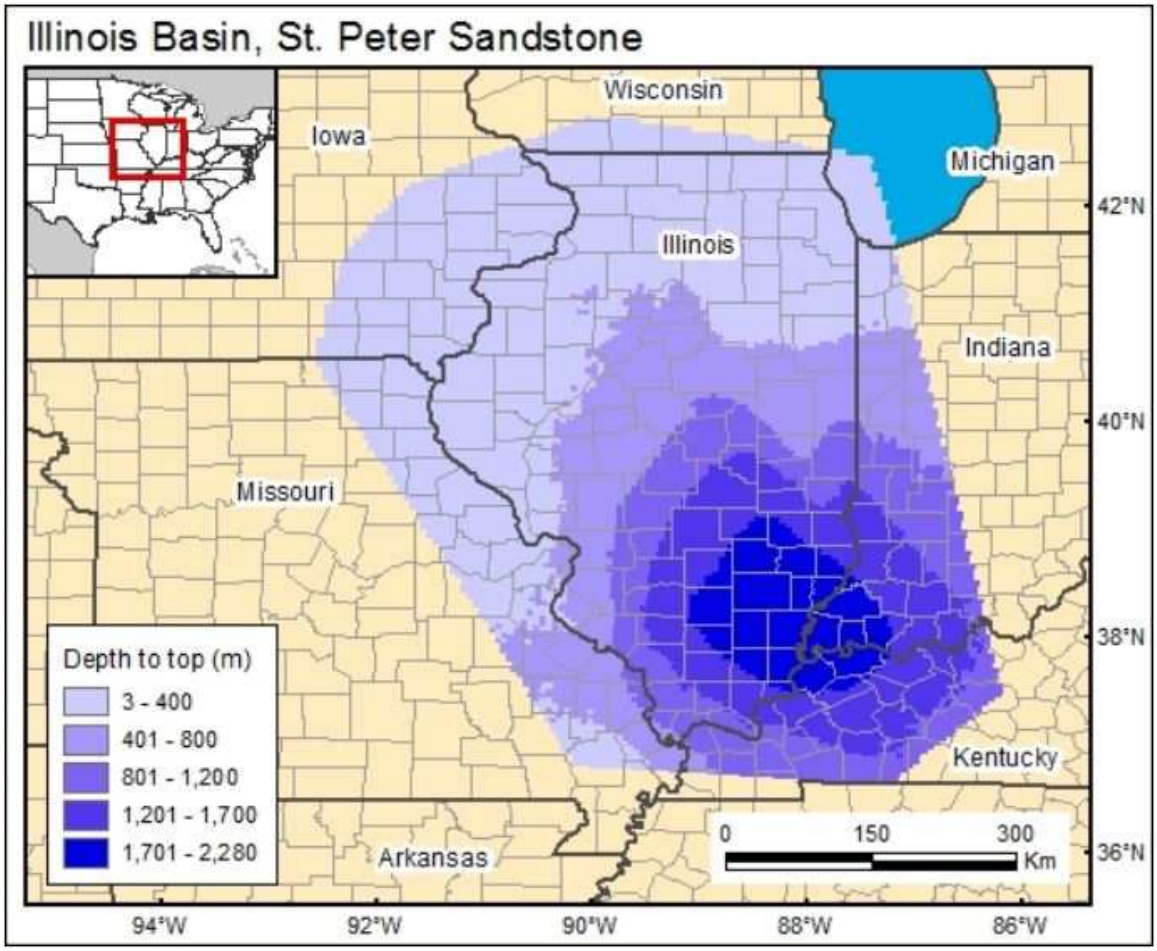

Fig. 13a: Depth to top of the St. Peter Sandstone in the Illinois Basin (Warne, 2012)

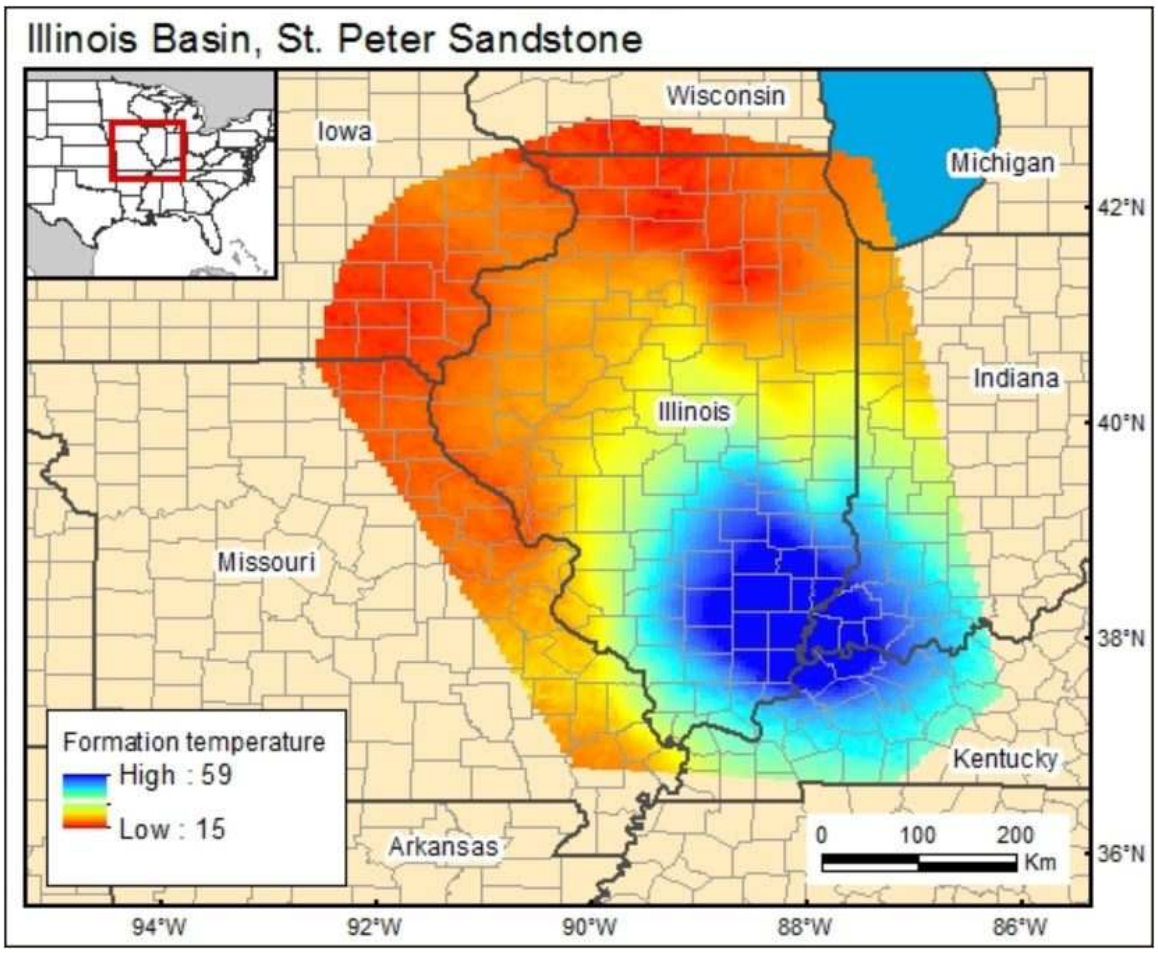

Fig. 13b: Estimated formation temperature of the St. Peter Sandstone in the Illinois Basin (Warne, 2012)

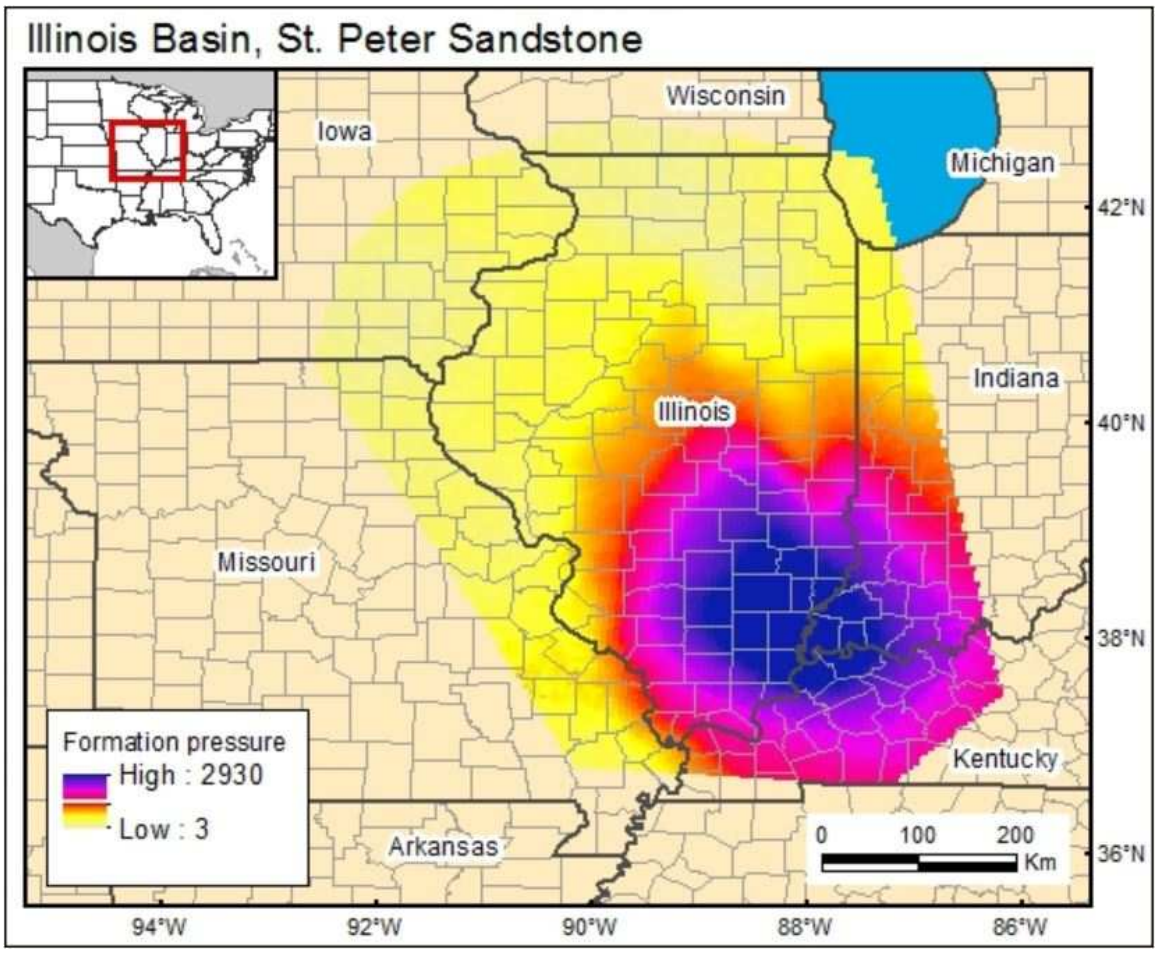

Fig. 13c: Estimated formation pressure of the St. Peter Sandstone in the Illinois Basin (Warne, 2012)

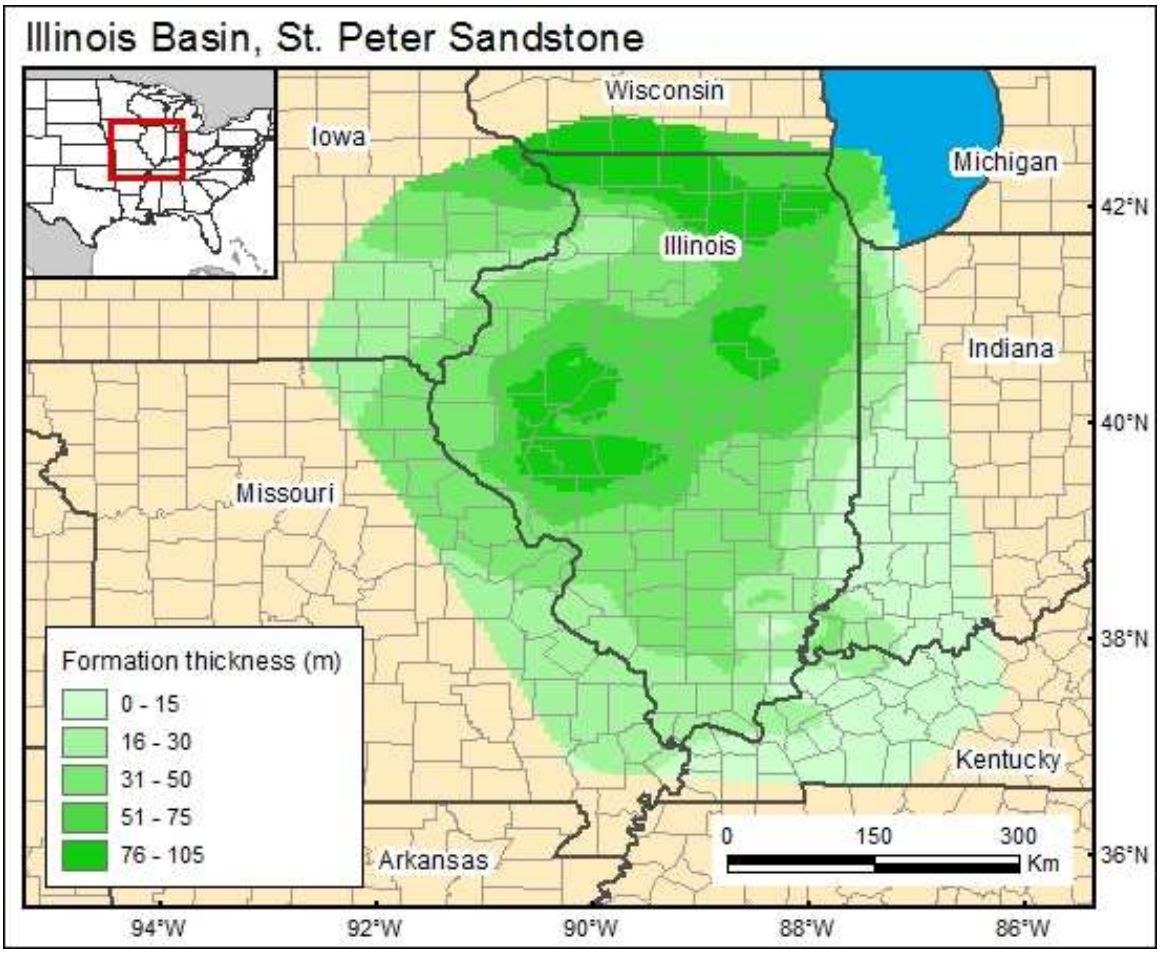

Fig. 13d: Estimated formation thickness of the St. Peter Sandstone in the Illinois Basin (Warne, 2012)

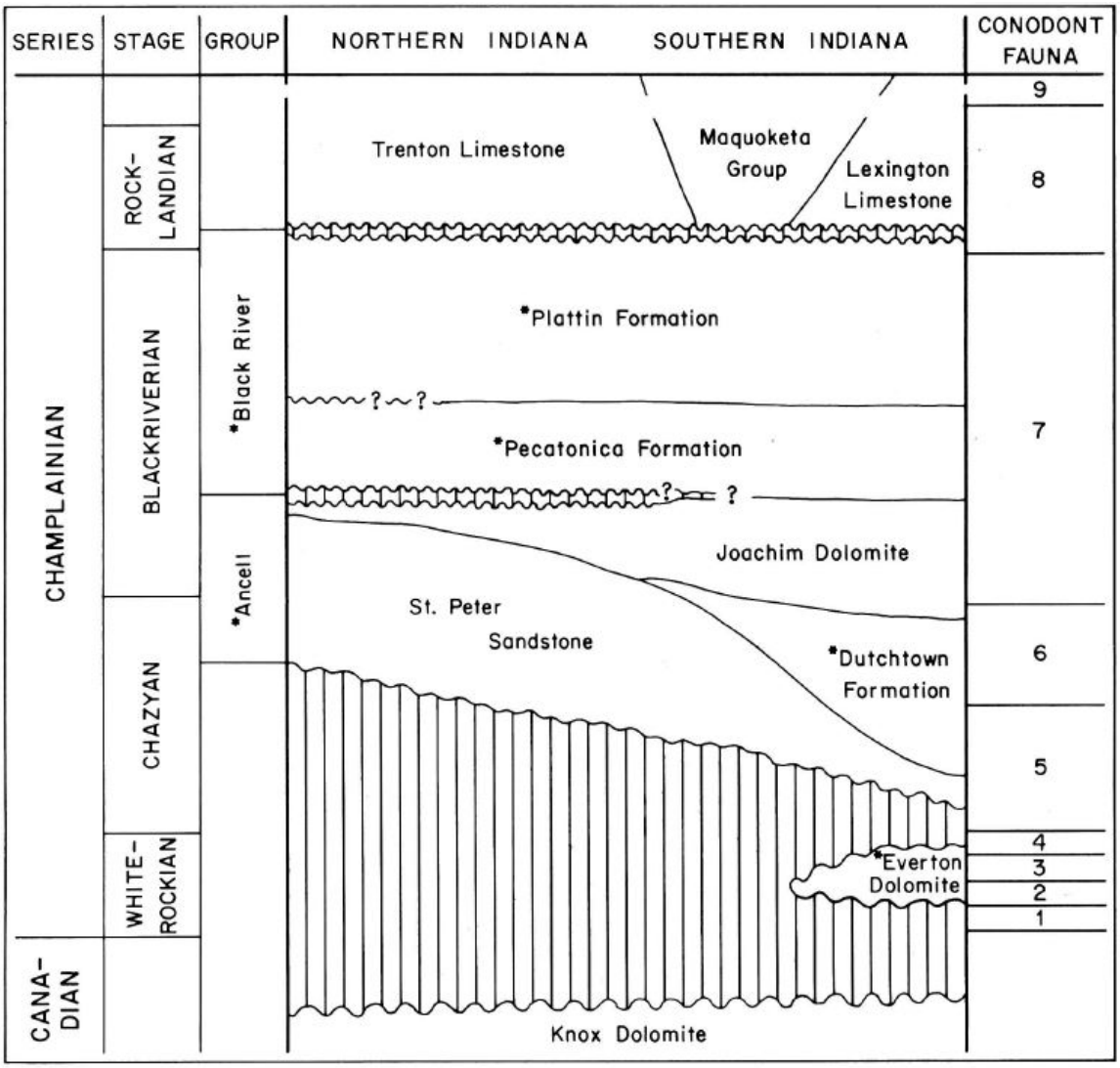

Fig. 14: Cross sectional map of the St. Peter Sandstone in the Illinois Basin (Droste, 1982)

B129 PRE-REACTION

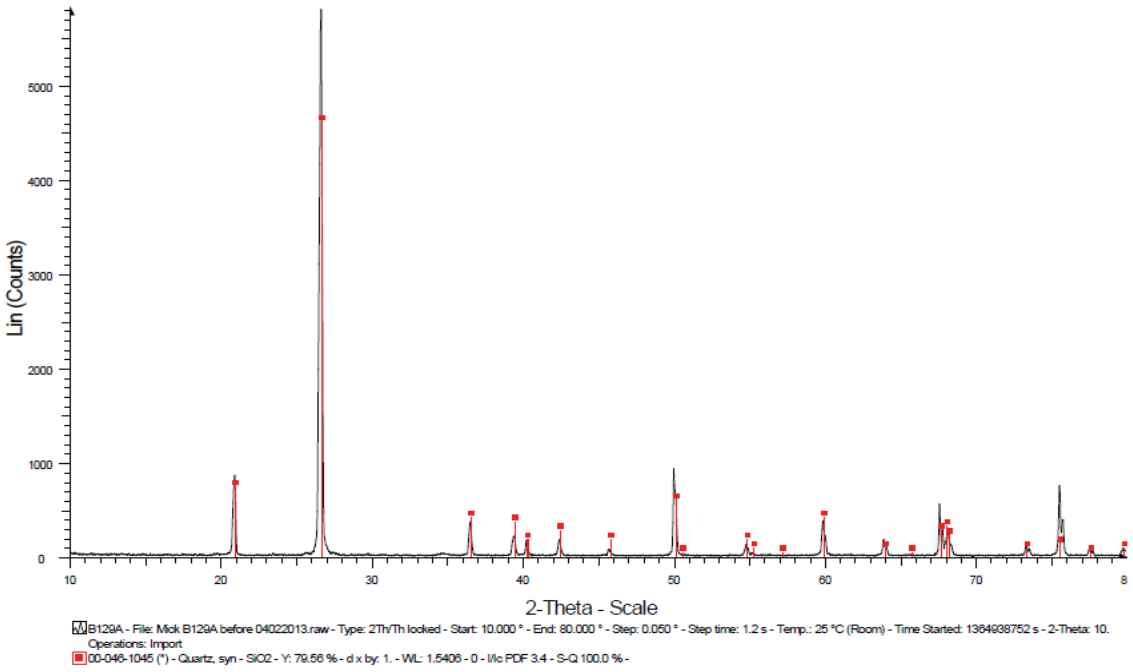

B129 POST-REACTION

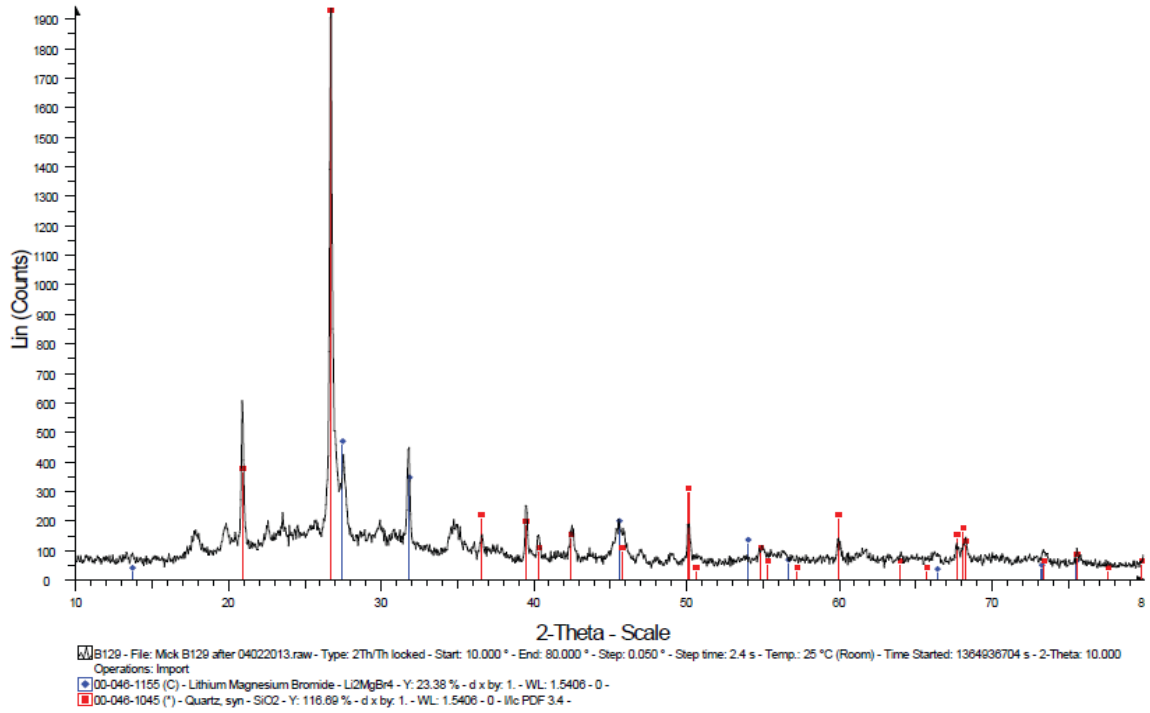

B131 PRE-REACTION

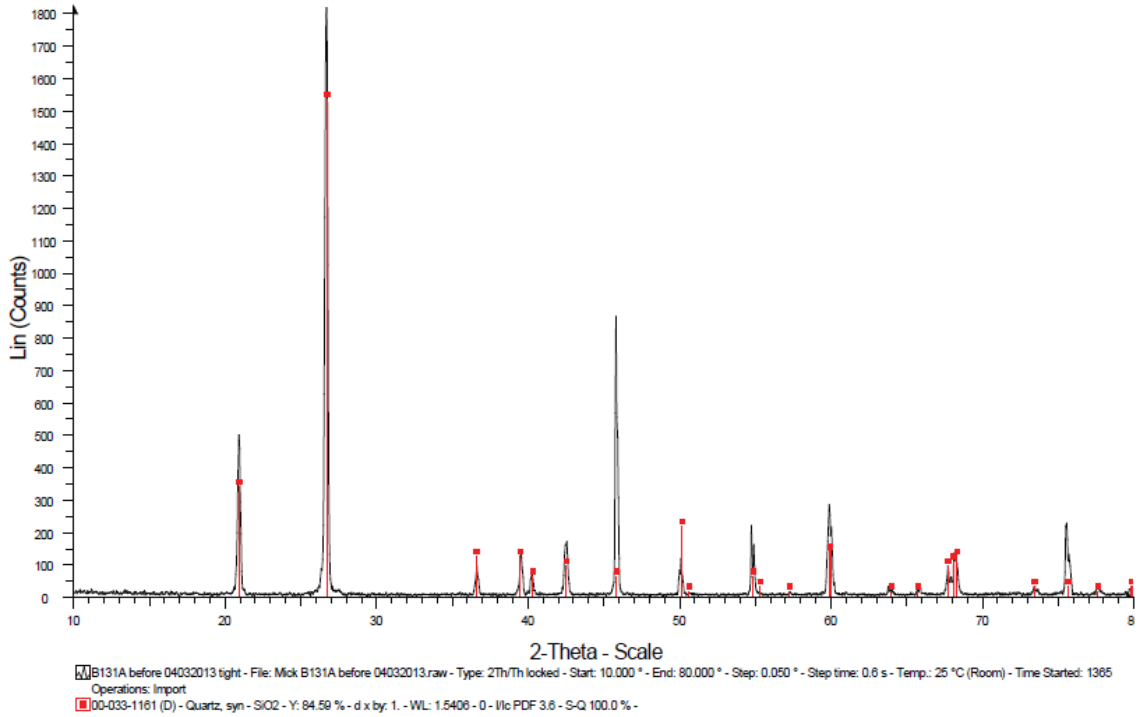

B131 POST-REACTION

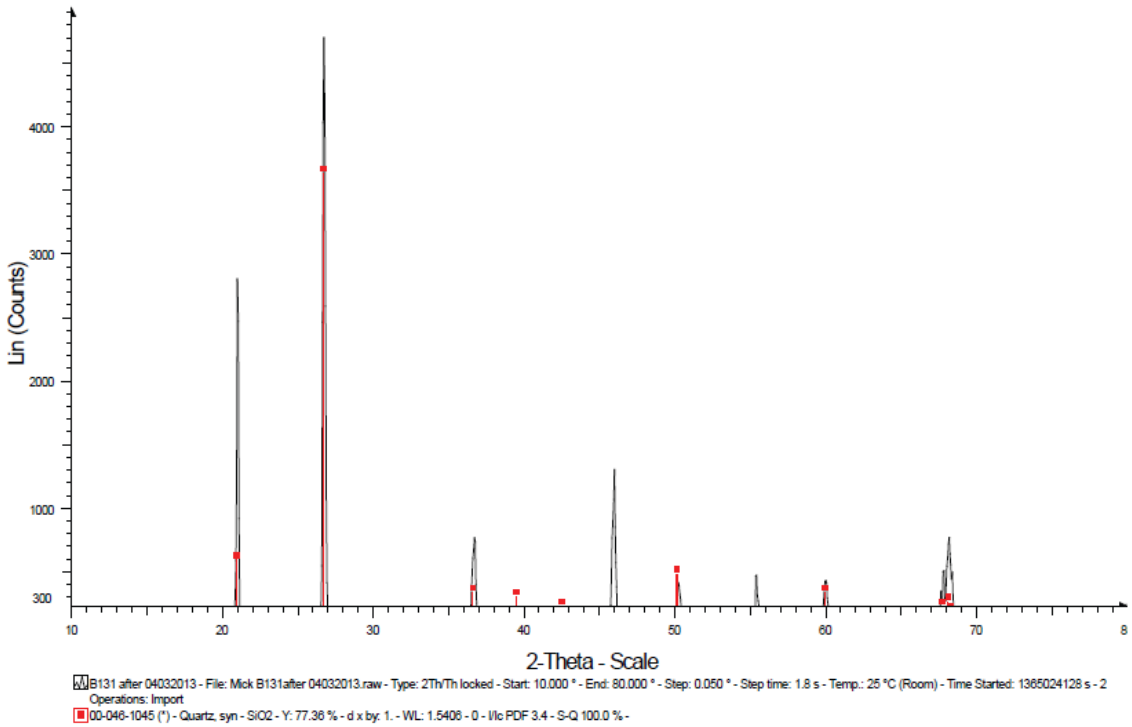

B137 PRE-REACTION

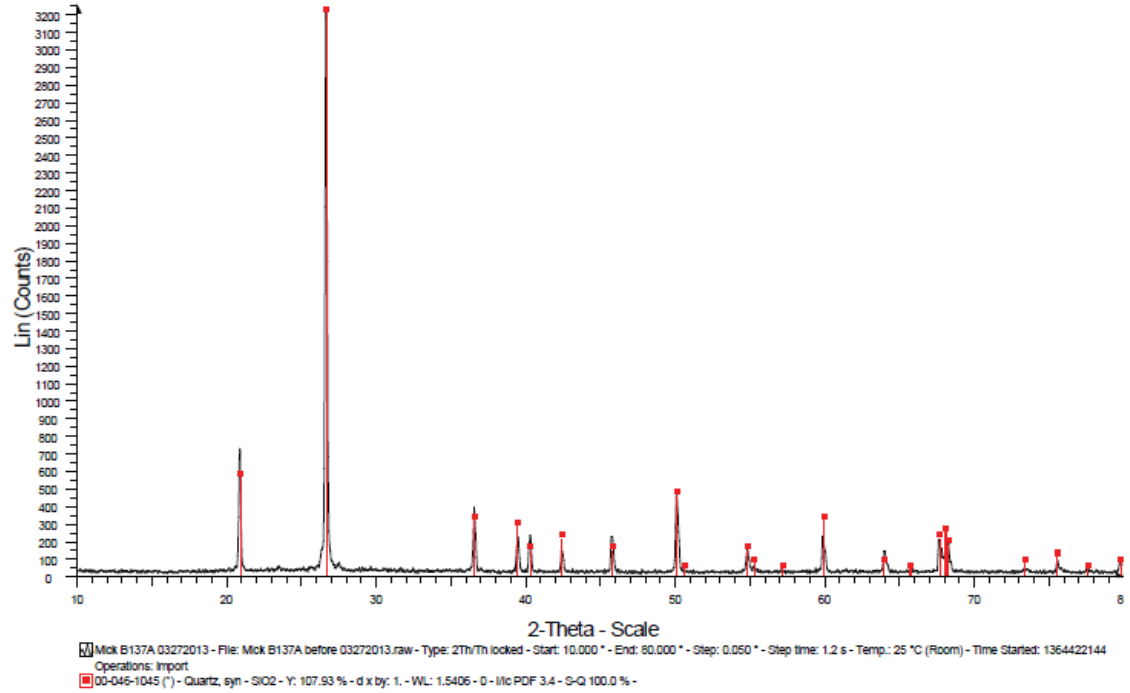

B137 POST-REACTION

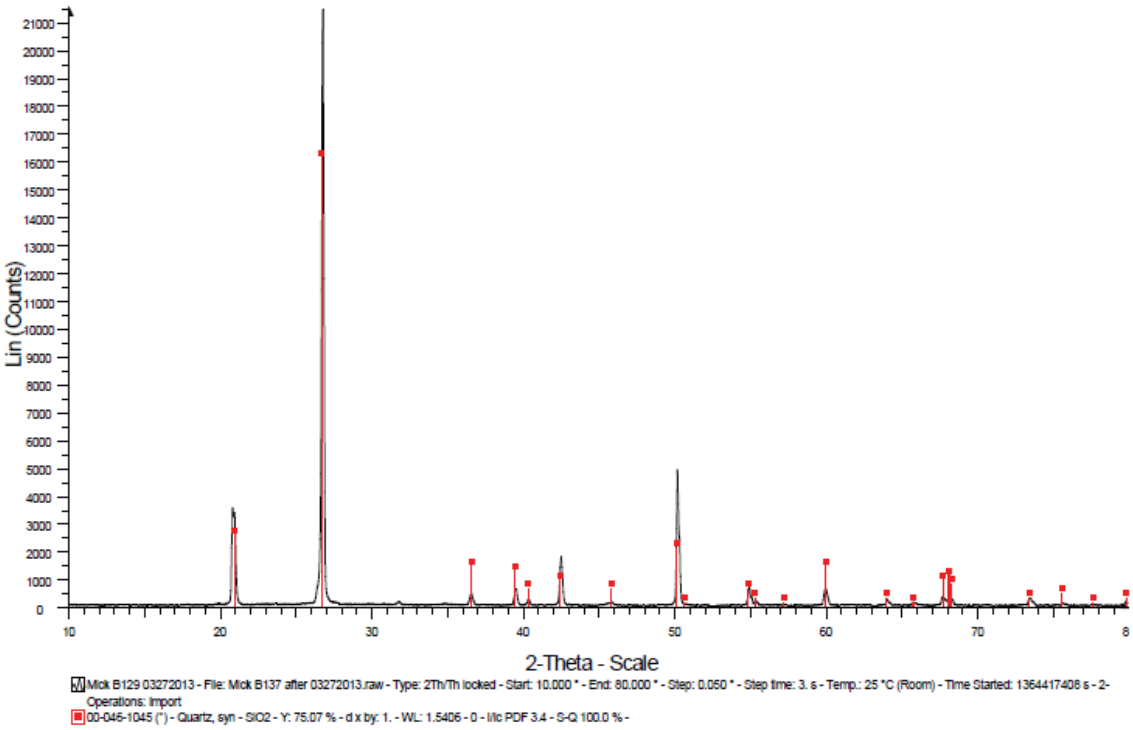

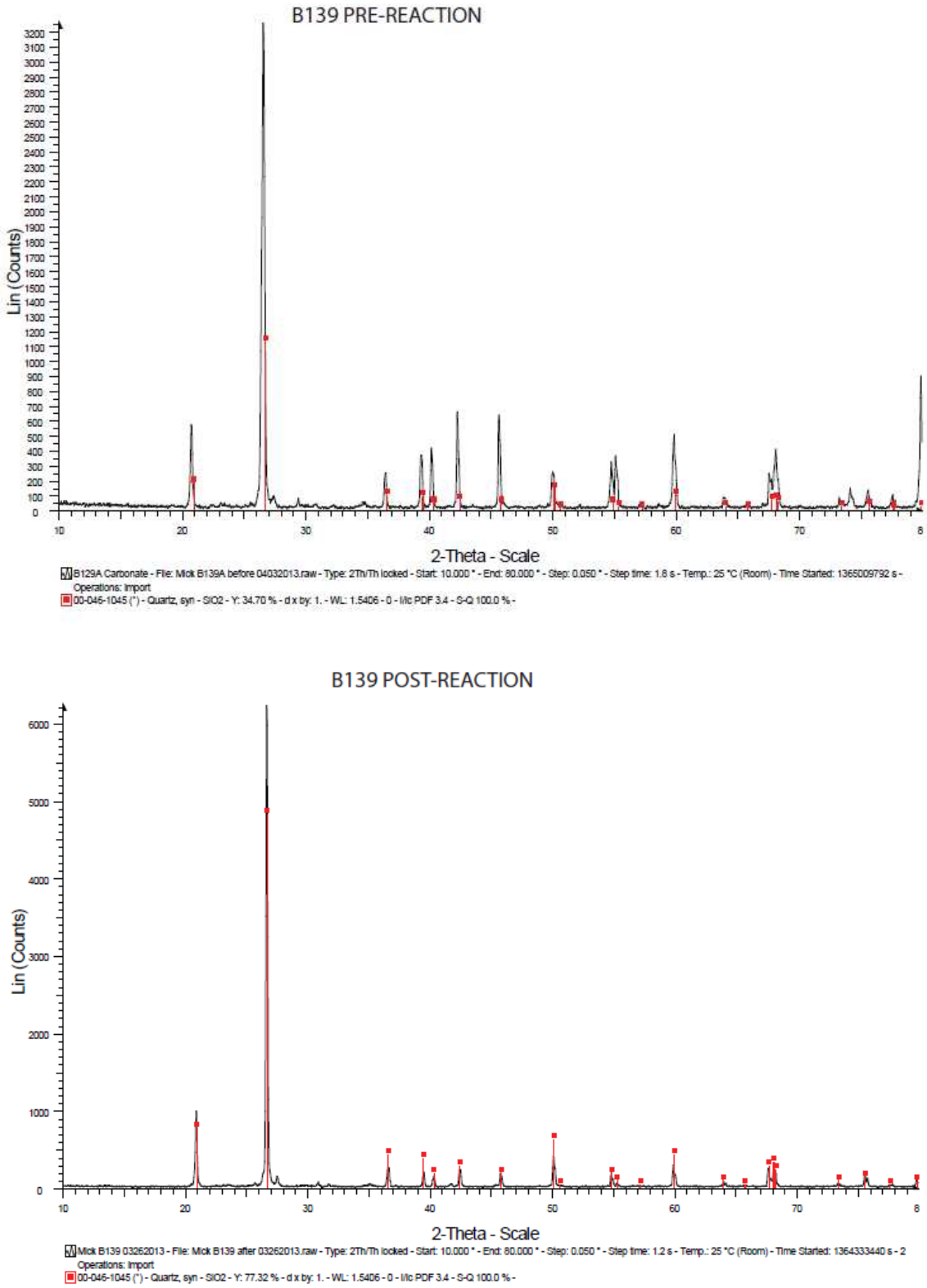

Fig. 15: X-Ray diffraction results.

REFERENCES CITED

Adebayo, T. A., 2013, Experimental Study of the Change in Porosity of Imeri Oilsand Rock Contaminated with CO_2: Chemical and Process Engineering Research, v. 16, p. 1-4.

Aguilera, R., 2002, Incorporating Capillary Pressure, Pore Throat Aperture Radii, Height above Free-Water Table, and Winland r_{35} Values on Pickett Plots: AAPG Bulletin, v. 86, no. 4, p. 605-624.

Ambrose, W. A., Lakshminarasimhan, S., Holtz, M. H., Núñez-López, V., Hovorka, S. D., Duncan, I., 2006, Geologic factors Controlling CO_2 Storage Capacity and Permanence: Case Studies Based on Experience with Heterogeneity in Oil and Gas Reservoirs Applied to CO_2 Storage: Environmental Geology, v. 54 p. 1619-1633.

Argonne National Laboratory, 2013, Total Porosity: http://web.ead.anl.gov/resrad/datacoll/porosity.htm (accessed December 21, 2013).

Bachu, S. K., 2009, Effects of In Situ Conditions on Aquifer Capacity for CO_2 Sequestration in Solution: www.netl.doe.gov/publications/proceedings/03/carbon-seq/PDFs/009.pdf (accessed May 6, 2013).

Ball, D., 2011, Midwest Regional Carbon Sequestration Project: http://addap.tk/userdata/phase_II_reports/phase_ii_final_report_MRCSP.pdf (accessed January, 2012).

Barnes, D., Lundgren, C., and Longman, M., 1992, Sedimentology and Diagenesis of the St. Peter Sandstone, Central Michigan Basin, United States: The American Association of Petroleum Geologist Bulletin, v. 76 p. 1507-1532.

Benson, S., and Cook, P., 2005, Underground Geological Storage: IPCC Special Report on Carbon dioxide Capture and Storage, p. 195-276.

Bentham, M., 2005, CO_2 Storage in Saline Aquifers: Oil & Gas Science and Technology, no. 3, p. 559-567.

Bergstrom, R.E., 1968, Feasibility of subsurface disposal of industrial wastes in Illinois: Illinois Geological Survey, Circular C 26, 18 p.

Berkey, C. P., 1906, Paleogeography of St. Peter Time: Geological Society of America Bulletin, v. 17, p. 229-250.

Bertier, P., Swennen, R., Laenen, B., Lagrou, D., Dreesen, R., 2006, Experimental identification of CO_2-water-rock interactions caused by sequestration of CO_2 in Westphalian and Buntsandstein sandstones of the Campine Basin (NE- Belgium): Journal of Geochemical Exploration, v. 89 p. 10-14.

Cartwright, K., Gilkeson. R. H., Griffin, R.A., Johnson, T.M., Lindorff, D. E., and DuMontelle, P. B., 1981, Consideration in hazardous waste disposal in Illinois: Illinois Geological Survey, Geological Note GN 94, 20 p.

Collinson, C., Sargent, M.L., and Jennings, J.R., 1988, Chapter 14: Illinois Basin region, *in* Sloss, L. L., ed., The Geology of North America, v. D-2, Sedimentary Cover-North American Craton: U.S.: Decade of North American Geology: Geological Society of America, p. 383-486.

Core Laboratories, 2012, Final Report [Core analysis study performed for Indiana Geological Survey]: Petroleum Services Division, Core Laboratories, 17 p.

Doughty, C., Pruess, K., Benson, S. M., Hovorka, S. D., Green, C. T., 2001 Capacity investigation of brine-bearing sands of the Frio Formation for geologic sequestration of CO_2. *in* Proceedings, 1st national conference on carbon sequestration, National Energy Technology Laboratory, Washington, DC, May 2001.

Droste, J.B., Abdulkareem, T., F., and Patton, J., B., 1982, Stratigraphy of the Ancell and Black River Groups (Ordovician) in Indiana, Occasional Paper 36, 15 p.

Egermann, P., Bemer, E., and Zinszner, B., 2006, An experimental Investigation of the Rock Properties Evolution Associated to Different levels of CO_2 Injection like Alteration Processes, *in* Proceedings, International Symposium of the Society of Core Analysts, Trondheim, Norway, September 2006.

Essendelft, D. V., 2005, CO_2 Sequestration through Deep Saline Injection and Photosynthetic Biological Fixation: System Design for Two Plausible CO_2 Sequestration Strategies: Department of Energy and Geo-Environmental Engineering, the Pennsylvania State University, 237 p.

Gaus, I., Azaroual, M., and Czernichowski-Lauriol, I., 2002, Reactive Transport Modeling of Dissolved CO_2 in the Cap Rock Base during CO_2 Sequestration (Sleipner Site, North Sea): French Geological Survey Open-File Report, 13 p.

Gaus, I., 2009, Role and impact of CO_2-rock interactions during CO_2 storage in sedimentary rocks: International Journal of Greenhouse Gas Control, vol. 4, p. 73-79.

Girard, J. R., and Barnes, D. A., 1995, Illitisation and paleothermal regimes in the Middle Ordovician St. Peter Sandstone, central Michigan Basin: K-Ar, oxygen isotope, and fluid inclusion data: American Association of Petroleum Geologists Bulletin, v. 79, p. 49-69.

Grabau, A. W., 1913, Principals of stratigraphy: New York, A. G. Seiler and Company, 1189 p.

Halliburton Inc., 2012, Calculating Fluid Saturations Using Leveret J-Functions: http://esd.halliburton.com/support/LSM/DSD/DSD/5000/5000_8/Help/mergedProjects/dsem/calculate_using_leverett_jfunctionsl.htm (accessed August, 2012).

Hoholick, D.J., 1980, Porosity, grain fabric, water chemistry, cement and depth of the St. Peter Sandstone in the Illinois Basin [Master's thesis]: University of Cincinnati, 72 p.

Hoholick, D. J., Metarko, T., and Potter, P. E., 1984, Regional variations of porosity and cement - St. Peter and Mount Simon Sandstones in Illinois Basin: American Association of Petroleum Geologists Bulletin, v. 68, p. 753-764.

Indiana Geological Survey, 2013, Potsdam Supergroup: http://igs.indiana.edu/compendium/comp0i04.cfm (accessed March 2013).

Izgec, O., Demiral, B., Bertin, H., Akin, S., 2008, CO_2 injection into saline carbonate aquifer formations I: laboratory investigation: Transport in Porous Media, v. 72, p. 1-24.

Jessop, P.G., and Leitner, W., 1999, Chemical Synthesis Using Supercritical Fluids: Weinheim, Wiley-VCH, p. 2.

Kaszuba, J.P., Janecky, D.R., and Snow, M.G., 2005, Experimental evaluation of mixed fluid reactions between supercritical carbon dioxide and NaCl brine: Relevance to the integrity of a geologic carbon repository: Chemical Geology, v. 217, p. 277-293.

Keller, S.J., 1983, Analyses of Subsurface Brines of Indiana: Indiana Geological Survey Occasional Paper 41, 37 p.

Kinney, D.M., 1976, Geothermal gradient map of North America: American Association of Petroleum Geologist and U.S. Geological Survey Publication G74014, scale 1:5 000 000, 2 sheets.

Leetaru, H.E., Rittenhouse, S.C., Frailey, S.M., Keefer, D.A., Morse, D.A., Finley, R.J., and McBride, J.H., 2005, National Energy Technology Laboratory, Deep Saline Reservoirs as a Carbon Sequestration Target in the Illinois Basin, *in* Proceedings, Fourth Annual Conference on Carbon Capture & Sequestration, Alexandria Virginia, May 2005.

Leone, J. A., 1988, Characterization and Control of Formation Damage ring Water flooding of a High-Clay Content Reservoir. SPE Reservoir Engineering, vol. 3, Number 4, p. 1279-1286.

Liu, F., Lu, P., Zhu, C., Xiao, Y., 2011, Coupled Reactive Flow and Transport Modeling of CO_2 Sequestration IN THE Mt. Simon Sandstone Formation, Midwest U.S.A.: International Journal of Greenhouse Gas Control, v. 5, p. 294-307.

Maroto-Valer, M.M., Druckenmiller, M.L., 2004, Understanding Carbonate Formation During Carbon Dioxide Sequestration in Saline Brine Formations: www.netl.doe.gov/publications/proceedings/04/carbon-seq/193.pdf (accessed August, 2012)

Mathis, R. L., Sears, S. O., 1984, Effect of CO_2 flooding on dolomite reservoir rock, Denver Unit, Wasson (San Andres) field, TX. *in* Proceedings, SPE annual technical conference and exhibition, Houston, TX, September 1984.

May, H., Dot Jr., R.H., 1985, A Subsurface Study of the St. Peter Sandstone in Southern And Eastern Wisconsin: University of Wisconsin-Extension Geological and Natural History Survey, Information Circular 47, p. 16-18.

Metz, B., Davidson, O., Coninick, H., Looz, M., Meyers, L., 2005, Intergovernmental Panel on Climate Change – Carbon Dioxide Capture and Storage: IPCC Special Report, U.K., Cambridge University Press, 230 p.

Mijic, A., 2013, Grantham Institute for Climate Change Near wellbore effects in CO_2 storage: http://www3.imperial.ac.uk/climatechange/research/sf/projects/mijic (access January, 2013).

Missouri St. Peter Sandstone, 2009, Missouri Department of Natural Resources: http://www.dnr.mo.gov/geology/geosrv/imac/stpetersandstone.htm (accessed October, 2011).

Mohamed, I., 2012, Carbon Dioxide Sequestration in Sandstone Aquifers: How Does It Affect the Permeability?: *in* Proceedings, Carbon Management Technology Conference, Orlando, February 2012, Section 2.5.1 Global Climate Change/CO_2 Capture and Management.

Nelson, P., 2009, Pore-throat sizes in sandstones, tight sandstones, and shales: The American Association of Petroleum Geologist Bulletin, v. 93 p. 329-340.

Nordbotten, J. M., Celia, M. A., Bachu, S., 2005, Injection and Storage of CO_2 in Deep Saline Aquifers: Analytical Solution for CO_2 Plume Evolution during Injection: Transportation in Porous Media, March 2005, Vol. 58, Issue 3, p. 339-360

Pitman, J.K., Goldhaber, M.B., and Spötl, C., 1997, Regional Diagenetic Patterns in the St. Peter Sandstone: Implications for Brine Migration in the Illinois Basin: U.S. Geological Survey Bulletin 2094-A, p. 1-20.

Pollington, A., Reinhard K., and Valley, J.W., 2011, Evolution of quartz cementation during burial of the Cambrian Mount Simon Sandstone, Illinois Basin: In situ microanalysis of Oxygen 18 Isotope: Geology, v. 39, p. 1119-1122.

Resource Investment Strategy Consultants, 2009, CO_2 Injection Well Cost Estimation: A.U. Commonwealth Department of Resources, Energy and Tourism, 17 p.

Ricardo, D. G., 2012, Effects of Dissolution on the Permeability and Porosity of Limestone and Dolomite in High Pressure CO_2/water Systems: Society of petroleum Engineers, Conference paper, SPE Annual Technical Conference and Exhibition, 8-10 October 2012, San Antonio, Texas

Rosenbauer, R. J., 2005 Experimental investigation of CO_2–brine–rock interactions at elevated temperature and pressure: Implications for CO_2 sequestration in deep-saline aquifers: Fuel processing Technology, vol. 86, Issues 14-15, October 2005, p. 1581–1597.

Roy, W.R., Mravid, S. C., Krapac, I. G., Dickerson, D. R., and Griffin, R. A., 1988, Geochemical interactions of hazardous wastes with geological formations in deep-well systems: Illinois Geological Survey, Environmental Geology Note EGN130, 52 p.

Schaper, J., 2011, Coverage of the St. Peter Sandstone in the U.S.: members.socket.net/~joschaper/sps.jpg (accessed March, 2012).

Solomon, S., 2007, Bellona Report, May 2007: Statoil Open-File Report, 128 p.

Soong, Y., Jones, J.R., Hedges, S.W., Harrison, D.K., Knoer, J.P., Baltrus, J.P., and Thompson, R.L., 2002, CO_2 Sequestration Using Brines: American Chemistry Society, Division of Fuel Chemistry, v. 47(1), p. 43-44.

Stephens, J.C., 2012, Carbon capture and storage Encyclopedia of Earth: http://www.eoearth.org/view/article/150922/ (accessed October, 2012).

Strąpoć, D., Mastalerz, M., Eble, C., and Schimmelmann, A., 2007, Characterization of the origin of coal bed gases in southeastern Illinois Basin by compound-specific carbon and hydrogen stable isotope ratios: Organic Geochemistry, v. 2 p. 267-287.

Swanson, B.F., 1981, A Simple Correlation between Permeabilities and Mercury Capillary Pressures: Journal of Petroleum Technology, v. 33, no. 12, p. 2498-2504.

Takahashi, M., 2005, Porosity increase Behavior in Persistent Compaction Regime of Stressed Sandstone: American Geophysical Union, Fall Meeting, San Francisco, California, Abstracts, p. A156.

Tsang, C., Birkholzer, J., Rutqvist, J., 2006, A comparative review of hydrologic issues involved in geologic storage of CO_2 and injection disposal of liquid waste: Environmental Geology, v. 54, Issue 8, p. 1723-1737.

Xu, T., 1999, Reactive Geochemical Transport Simulation to Study Mineral Trappings for CO_2 Disposal in Deep Saline Arenaceous Aquifers: Earth Sciences Division, Lawrence Berkeley National Laboratory, University of California, Berkeley, CA 94720, 66 p.

Xu, T., 2004, CO_2 Sequestration in Bedded Sandstone-Shale Sequences: Earth Sciences Division, Lawrence Berkeley National Laboratory, University of California, Berkeley, CA 94720, 10 p.

Warne, A., 2012, Bureau of Economic Geology, University of Texas at Austin, St. Peter Sandstone, Illinois Basin: http://www.beg.utexas.edu/environqlty/co2seq/co2data/0stpeter.htm (accessed March, 2012).

Young, H.L., 1992a, Summary of ground water hydrology of the Cambrian-Ordovician aquifer system in the northern Midwest, United States: U.S. Geological Survey, Professional paper 1405-B, 99 p.

CURRICULUM VITAE

Richard Michael Thomas

Education

- M.S. Geology – Indiana University

Honors, Awards, Fellowships

- AAPG Imperial Barrel Award Team, Founder and Team Lead
- Presidential Management Fellow

Research and Training Experience

- Basin analysis of the Guadalupe Mountains: Permian Basin. Funding provided by Exxon Mobil
- Impact of CO2 injection on microbial population in hydrocarbon reservoir - Sugar Creek Field, Western Kentucky. Funding provided by the KYGS
- IUGFS Field Camp, Summer 2011

Professional Experience

- ALS Empirica; Houston/U.S. Rockies - Field Geologist
- Horizon Well Logging and Geosteering LLC; Tulsa OK - Geologist
- Indiana University Purdue University Indianapolis; Indianapolis, IN – R.A., T.A., Lab Technician
- Dubric LLC; Comstock MI – Rotating Equipment Specialist
- Endress + Hauser; Greenwood IN – Engineer
- PamLab LLC; Covington LA – Pharmaceutical Sales
- ProNet LLC; St. Charles MO – Chemical Sales

- Dema Engineering INC; St. Louis MO – Applications Engineer

Conferences Attended

- Indiana University Crossroads Conference, Bloomington – 2011, 2012
- AAPG Eastern Regional Conference, Cleveland OH – 2012
- AAPG Student Expo, Pittsburg PA – 2012
- GSA National Conference, Charlotte NC – 2012
- Illinois Oil and Gas Association Annual Conference, Evansville IN – 2014

Publications

Geochemical impact of supper critical CO_2 injection into the St. Peter Sandstone formation within the Illinois basin.